An archaeometric investigation of early and middle bronze age pottery from the upper meander basin in southwestern anatolia

5 authors, including:

Baris Semiz
Pamukkale University
21 PUBLICATIONS   **38** CITATIONS

Some of the authors of this publication are also working on these related projects:

Project   CLAY RESOURCES AND TECHNICAL CHOICES FOR ANTIQUE POTTERY IN DENİZLİ REGION: MINERALOGICAL, CHEMICAL, AND TECHNOLOGICAL ANALYSES View project

AN ARCHAEOMETRIC INVESTIGATION OF EARLY AND MIDDLE BRONZE AGE POTTERY FROM THE UPPER MEANDER BASIN IN SOUTHWESTERN ANATOLIA

Barış Semiz[1], Eşref Abay[2], Fulya Dedeoğlu[2], Erim Konakçi[3] and Ali Ozan[3]

[1]Pamukkale University, Department of Geological Engineering, 20020 Denizli, Turkey
[2]Ege University, Department of Archaeology, İzmir, Turkey
[3]Pamukkale University, Department of Archaeology, 20020 Denizli, Turkey

ABSTRACT

We present the results of a comprehensive mineralogical and geochemical (archaeometrical) investigation of ceramics dating to the Early Bronze Age II (2600/2500-2200 BC) and the Middle Bronze Age (2000-1600 BC) from sites located in the Upper Meander Basin of Denizli province in southwestern Anatolia. We analyzed the mineralogical and petrographical characteristics of the samples using X-ray diffraction (XRD) and optical microscopy, and we examined the chemical compositions with X-Ray Fluorescence (XRF). In general, the primary components of the ceramics include coarse-grained quartz, biotite, muscovite, pyroxene, plagioclase, and metamorphic rock fragments; we estimate a firing temperature under 800°C. The ceramics appear to be locally manufactured, given the close relationship between their mineralogical properties and the local geological structure and topography. Our analysis indicates that people living in the mountainous, plateau, and lowland areas each preferred different clay deposits in their pottery production. All of these areas, however, shared similar production technologies.

1.   INTRODUCTION

The main database for this study consists of petrographic thin sections of ceramic samples dating to the Early Bronze Age II (2600/2500-2200 BC) and Middle Bronze Age (2000-1600 BC) from the Upper Meander Basin in southwestern Anatolia. Ceramics from this period have previously received significant archaeological attention at the macroscopic level (Lloyd and Mellaart, 1962, 1965; Abay and Dedeoğlu, 2009; Dedeoğlu 2013, 2016; Dedeoğlu et al., 2016). In the surrounding regions, the ceramics from contemporary settlements have also undergone archaeometric analysis, often combining chemical and mineralogical studies (Day et al., 2009 at Liman tepe and Bakla tepe; Brunelli et al., 2013 in the Aeolian Islands; Türkteki, 2014 at Küllüoba, Eskişehir; Kibaroğlu and Hartmann, 2015 in northeast Syria and southeast Anatolia; Belfiore et al., 2007 in Haghia Triada, Crete; Luke et al., 2015 in the Gediz River Valley; Kılıç et al, 2017 in Tilkitepe; Javanshah, 2018 in Shahr-I-Sokhta; Sarhaddi-Dadian et al 2015 in Sistan (Iran) and Pourzarghan et al., 2017 in Eastern Iran). In these studies, the analysis of the components of the ceramic samples led to inferences concerning the sources of raw materials and the organization of production. For example, Türkteki (2014) combined chemical, statistical, and petrographic analyses of ceramics to evaluate early attempts at standardization in the Early Bronze Age (EBA) pottery production of western Anatolia. Luke et al., (2015) combined a variety of archaeometric techniques in order to uncover valuable insights into the continuity and change of ceramic recipes in western Anatolia during the transition from the Late Bronze Age (LBA) to the Iron Age (Luke et al., 2015). However, these types of data-intensive studies remain challenging to carry out, given current impediments to data access and sharing at the larger inter-regional scale, though the number of such studies has been increasing in recent years.

Building on these examples, our research applies a variety of analytical approaches to the ceramic evidence in order to explore the social practices of Bronze Age southwestern Anatolia. In terms of morphology, the ceramics of the Upper Meander Basin are relatively homogeneous across a broad area during both the EBA II and Middle Bronze Age (MBA). The first question of this study addresses whether these homogeneities of form across settlements in varied topographies and geological units are paralleled by commonalities in the manufacturing methods as confirmed by archaeometric analysis. In particular, do the settlements of the basin lowlands, often considered the center of human activities, differ from the mountainous and plateau-based settlements, usually considered secondary and rural, in terms of ceramic production? Or, was common knowledge about ceramic technology widespread around the entire region, reflecting a high level of integration as seen in the macroscopic comparisons of the survey material? Moreover, our research seeks to determine, for each subregion, the characteristics of the raw materials used in ceramics manufacturing, as well as the specifics about the production techniques, such as the use of kiln drying. The dataset analyzed in our study includes ceramic samples selected from each macroscopic ware group identified at the settlements of the lowland, plateau, and mountainous areas of the Basin from our periods of interest. This represents the first detailed archaeometric study of material from the EBA and MBA in the Upper Meander Basin.

2.   ARCHAELOGICAL CONTEXT

The Upper Meander Basin sits completely within the borders of Denizli province, at an altitude of 800-850 meters and has an area of 815.6 km². The combined geographical area of the mountains and plateaus, surrounding and including the Basin, totals 1426 km². The Basin is situated on a number of natural transportation routes among the surrounding regions. To the northeast, it connects with the Sandıklı (Afyon) plain (Sandıklı - Afyon Ovası) via the Küfü Stream and the Düzbel Pass. To the north lays the Uşak plateau and to the east is the natural route to Dinar and the Lakes region (Göller Yöresi). Several water sources irrigate the broad plains of the Basin, including the Küfü Stream to the northeast. The most significant water source, however, is the Meander River, which is the largest river in the Aegean region (Ceylan, 1998). This area also contains lakes and desiccated lake beds.

Intensive archaeological surveys of the Basin, begun in the 1950s and resumed between 2003-2015, have recorded significant inhabitation since at least the Neolithic Age (Lloyd and Mellaart, 1962; 1965; Abay and Dedeoğlu 2009; Abay 2008; Dedeoğlu, 2013; Dedeoğlu et al., 2016). These research programs have mapped over 250 archaeological settlements in the Basin. Significant sites currently under excavation include Ekşi Höyük, with layers dating to the Neolithic, Early and Middle Chalcolithic periods, and Beycesultan Höyük, with layers from the Late Chalcolithic, Early, Middle and Late Bronze Ages, the Iron Age, and the Byzantine and Seljukian periods.

The Basin appears to have witnessed increasingly complex social organization during the EBA II and MBA. Beginning in the EBA, we observe a dense population of people living varied modes of life in the lowlands, the mountainous areas, and on the

plateaus of the Basin. We note in particular the emergence of single-period hilltop settlements of the EBA II, usually situated among the foothills of mountainous areas. These settlements, which show a regular pattern of dispersal in the foothills, have a similar ceramic culture with the lowland settlements in terms of forms and manufacture quality. Thus, we propose that the Upper Meander Basin attracted settlement in the EBA II with new settlements being located at the same time in all topographical regions: the lowlands, the mountainous areas, and on the plateau. Although some EBA II ceramic ware groups exhibit more elaborate workmanship and production technology, clear evidence for ceramics specialization is generally lacking.

The innovation of the potter's wheel entered the Basin during the EBA III period, similar to the surrounding regions of western Anatolia. Specialization in ceramic production becomes even more apparent in the MBA and the LBA. Written sources of the LBA suggest that the Basin was part of the Arzawan Kingdoms (Hawkins, 1998). The organization of a kingdom in the Basin may have impacted ceramic production technologies and traditions, together with other social structures. New types of buildings found at Beycesultan Höyük, such as palaces, public buildings, temples, and elite houses, may indicate this settlement's political and economic centrality during the Arzawan period (Lloyd and Mellaart, 1962; 1965; Dedeoğlu, 2013).

In summary, the overall trend we observe from the combined archaeological evidence is an increase in the social complexity of settlements in the Upper Meander Basin beginning in the EBA. Our goal is to investigate how these changing social structures im-

pacted the material culture in general and the production of pottery in particular. We study pottery production decisions using an archaeometrical analysis of sherds that were sampled from a range of settlement types, sizes, and topographical situations.

3. MATERIALS AND METHODS

Ceramic samples were selected for analysis from 11 settlements of the lowland, the plateau, and the mountainous areas of the Basin (Table 1 and Appendix 1 and 2). Samples found during surface survey come from the settlements of Aşağı Asar Tepe, Kocakaya, İlımanlı, Belkuyu, Çeşmebaşı, Cabar Asartepe, Göceler, Höyük, Asmakuyu Tepe and Kocainüstü (Dedeoğlu et al., 2016). Excavation samples were recovered from the ongoing project at Beycesultan Höyük (Abay 2008; Abay and Dedeoğlu, 2009) (Appendix 1; Fig. 1). We selected a total of 49 ceramic sherds of the EBA II and MBA based on their macroscopic characteristics and representativeness of periods and types (Appendix 2). The thin sections of these 49 samples were petrographically investigated at the Department of Geological Engineering of Pamukkale University (PAÜ). The thin sections of the samples were cut perpendicular to the vessel wall in order to examine every layer from the exterior to the interior. The mineralogical and petrographical characteristics of the samples were studied using a Leica (DM750) polarizing microscope at the Department of Geological Engineering. As a result of the polarizing microscope examination, some samples from the same petrographical groups were chosen for further investigation with other techniques.

Table 1. Location, chronology, topographic situation and the number of analysed samples.

Location	Abbv.	Period	Topographic situation	Samples
Beycesultan Höyük	BHY	EBA-II	Lowland	E01, E02, E03, E04, E05
Aşağı Asartepe Settlement	AAS	MBA	Mountainous	E06, E07
Kocakaya Settlement	KS	MBA	Mountainous	E08, E09, E10, E11
İlimanlı Höyük	IH	MBA	Mountainous	E12
Belkuyu Höyük	BH	MBA	Mountainous	E13, E14, E15
Çeşmebaşı Settlement	ÇS	MBA	Mountainous	E16, E17, E18
Cabar Asartepe Settlement	CAS	MBA	Mountainous	E19, E20, E21
Göceler Höyük	GH	MBA	Plateau	E22, E23, E24,
Höyük Settlement	HS	MBA	Lowland	E25, E26, E27, E28, E29
Asmakuyu Tepe Settlement	ATS	EBA-II	Mountainous	E30, E31, E32
Kocainüstü Tepe Settlement	KTS	EBA-II	Mountainous	E34, E35
Beycesultan Höyük	BYH	MBA	Lowland	E36 between E49

Twenty-one representative samples were chosen for X-ray Fluorescence. We measured for all major rock minerals and some trace elements, and we made readings on fresh bulk samples extracted from

within the sherds at sufficient quantities for measurement. These readings were made at the Department of Geological Engineering at Pamukkale University using a Spectro XEPOS Polarized Energy

Dispersive X-ray Fluorescence spectrometer (PEDXRF). This instrumentation has a 50 W Pd end-window X-ray tube with a spectral resolution of 160 eV (1000 cps Mn Kα). When taking measurements, we flushed the sample chamber with Helium. We made use of United States Geological Survey (USGS) standards to calibrate the XRF machine, including the sediments identified as GEOL, GBW-7109 and GBW-7309. Samples were crushed in a tungsten carbide crushing vessel, and then 6.25 g of powdered sample was separated and mixed with 1.4 g of wax (M-HWC). An automatic press with a force of 18N pressed this mixture into a disc.

From among the samples selected for XRF, we also subjected ten to X-ray powder diffraction (XRD) analysis. This method can identify all mineral phases, including the smallest-grained components that are not observable with a microscope. The mineralogical composition of 10 samples was determined with XRD (Co$_{Kα}$1 radiation, λ=1.7889 Å, 40 kV and 30 mA) using an Inel Equinox 1000 in the Department of Geological Engineering at Ankara University. In a tungsten carbide crushing vessel, we ground these samples into a fine powder and then placed a few milligrams into sample holders for use in the XRD machine. We recorded diffraction patterns at a scanning rate of 0.02 degrees per second in 2θ ranging from 2°-70° in bulk-sample diffractograms. A search-match software program aided our phase identifications. This XRD analysis provided estimates on semi-quantitative percentages based on the external standard method.
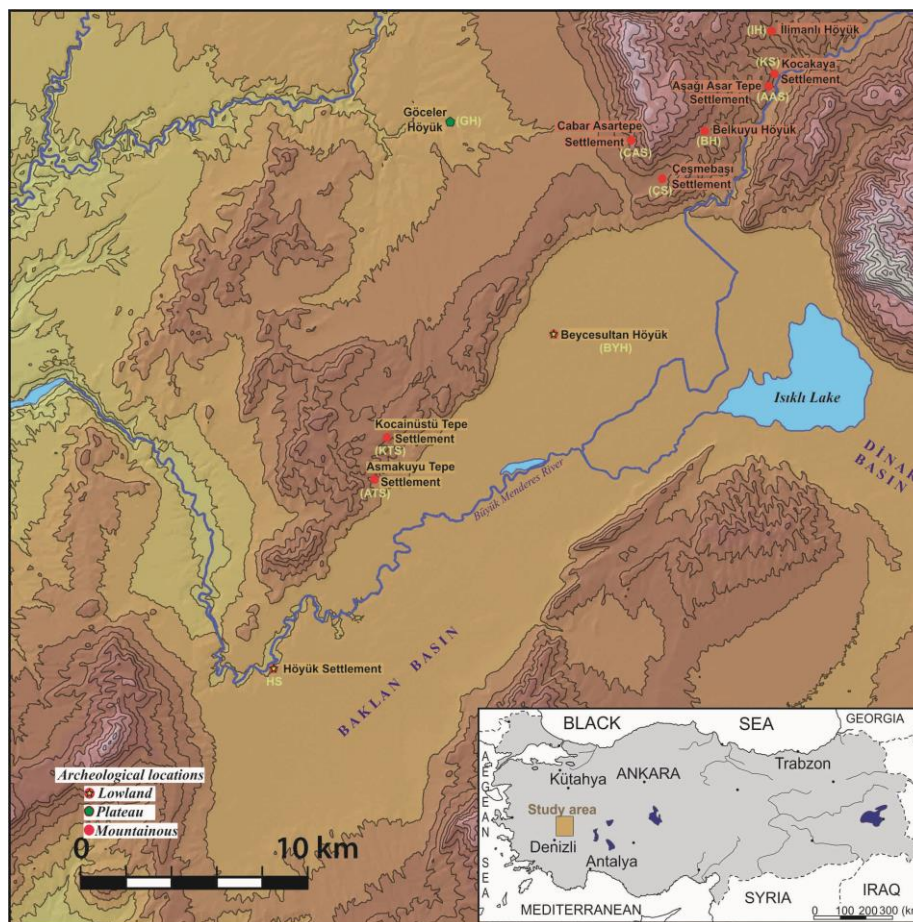
Figure 1 Digital Elevation Model (DEM) and topographical map of the prehistoric archaeological sites of the Upper Meander Basin.

4. GEOLOGICAL FEATURES OF THE STUDY AREA

The Çivril Graben System is a wide sedimental plain, almost 100 km in length, and composed of two main parts, the Baklan and Dinar Basins. These two basins take the shape of a south-facing bow with ends pointed towards the southwest and southeast (Özalp et al., 2009). Both sides of the southwest-northeast trending Baklan Basin and the northern side of the northwest-southeast trending Dinar Basin have active faults. The configuration of a fault on the southern side of the Dinar Basin is uncertain in contemporary morphological understanding. The faults of the Baklan and Dinar Basins are composed to the west of metamorphic rocks from the Menderes Massif, to the north of metamorphic rocks from the

Afyon zone, and to the east and most southern parts of units of the Lycia nappes (Fig. 2).

The base geology of the study area and the surrounding Meander Massif consists of Paleozoic-Early Tertiary aged schist (garnet schist, garnet mica schist, biotite schist), quartzite and marble bands, and lenses that show low degree metamorphic features with a diversity of mineralogical paragenesis. The upper layers of this region are represented by calcschist and chlorite schists (Konak et al., 1986; Dora et al., 2001; Konak, 2002). The Afyon zone north of the study area consists of Paleozoic low degree metamorphic rocks that can be divided into Lower and Upper metamorphic units. The Lower metamorphic units are composed of rocks such as quartzites and porphyroids and the Upper metamorphic units are composed of rocks such as metaconglomerate and metapelitic (Tolluoğlu et al., 1997; Ay et al., 1999). The Porphyroid type of rocks are known as a metamorphosed felsic volcanic (meta-rhyolites) unit (Tolluoğlu and Sümer, 1997). These rocks are most likely the result of intraplate magmatism in a period that follows the metamorphism of the lower metamorphic rocks in the Middle Cambrian (Tolluoğlu et al., 1997). The Lycia nappes include different sequences and tectonic units formed under a variety of environmental circumstances. Overlapping structures reach the continental slope deposits, and separate ophiolite and volcano sedimentary units form the upper layers of the nappes (Graciansky, 1972; Yılmaz et al., 2000). The nappes overlap the Meander Massif allochthonously and start with metaclastic rocks that turn into limestones towards the upper layers. The Metaclastic rocks start with yellowish, brownish mostly bright white quartz graveled metaconglomerates and continue with arkosic meta sandstones and meta siltstones in sequence (Konak et al., 1986).

Molasse qualified, Oligocene conglomerates overlap the geological units described above in an unconformable way. They outcrop in wide areas on the southern and southeastern parts of the Baklan and Dinar Basins. On top of these basic units, Late Miocene-Pliocene lacustrine sediments and river products composed of sandstones, siltstones, mudstones, marls and limestones are deposited by angular unconformities. The Miocene-Pliocene units include lignite levels with economic reserves (Altay and Dumlupınar, 2013; Akkiraz et al., 2006). Along the northern border of the Basins, carbonate cemented conglomerates uncomformably overlap the base rocks. In the Basins, river-lacustrine units contain conglomerate sequenced by mudstones, marls and siltstones. Plio-quaternary units deposited under the control of active tectonism are constituted by alluvial fan and river-lacustrine sediments.
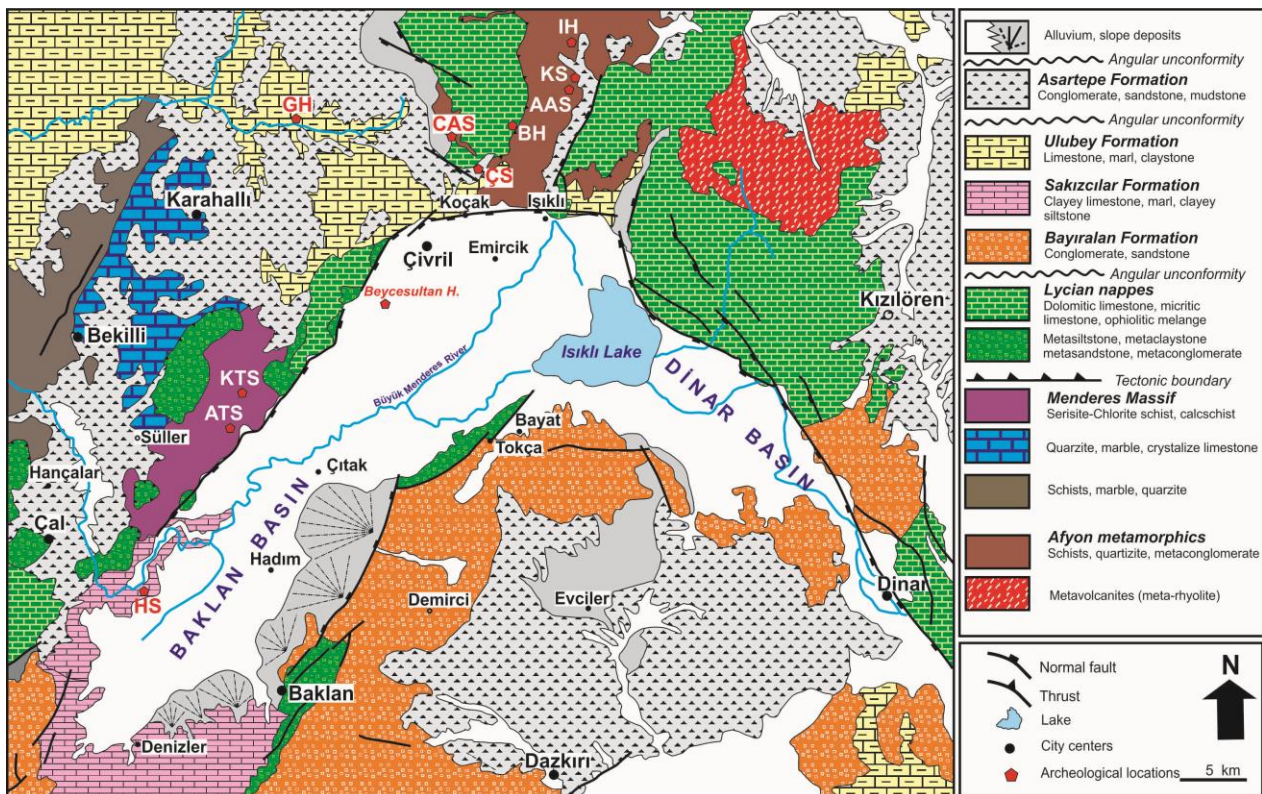
Figure 2 Generalized geological maps of the Upper Meander Basin (Çal-Çivril-Baklan area). (Abbreviations for mountain, plateau, and lowland settlements based on Fig. 1)

5. RESULTS

5.1. *Petrographical analyses*

We followed the methodology suggested by Kibaroğlu et al., (2011) and Carvajal López and Day (2015) in our petrographic analyses. Almost all of the ceramic samples from the prehistoric settlements of the Upper Meander Basin are composed of coarse-grained, angular and semi-angular grains of minerals and rocks whose dimensions vary between silt (0.02 mm) and sand (1-2 mm). The ceramic samples form 3 groups according to the quantities of rock fragments and mineral types included in each matrix.

In all samples, the main rock fragments consist of metamorphic rocks with a variety of components (quartzite, mica schist, muscovite schist, etc.). The mineral fragments in the samples include quartz, biotite, muscovite, pyroxene, calcite, and plagioclase, in varying quantities (Fig. 3). The general colors of the pottery samples range from brown to black, with some samples exhibiting bichromatic dark brown-black and reddish matrices. Several samples have the typical light-edge to dark-core transition characteristic of varied oxidation due to contact with the atmosphere at a low temperature ratio. This property usually indicates an extended period of kiln drying (Nodari et al., 2004; Maritan et al., 2006; Semiz and Duman, 2017). Some samples are also characterized by a high percentage of porous area (up to 35%). These voids range from wide to narrow, and sometimes exhibit a preferred orientation. In the following section, we summarize the specific differences observed among the three petrographic groups.

Group 1: This group of 11 sherds is characterized by abundant carbonates, with few rock fragments, and few quartz and muscovite minerals. For example, the carbonates in sample E04 from Beycesultan include monocrystalline calcite, averaging around 0.6 mm in length. In most samples in this group, the few rock fragments generally include quartz-muscovite schist and smaller amounts of quartzite gravel. These fragments have less quartz than average rocks of these types and the grains are angular and semi-angular in shape. These grains are scattered in the matrix, taking up only about 5% of the area. The samples contain even less pyroxene, plagioclase and biotite minerals. Muscovite is more abundant in sample E02 (Fig. 3a), which also has pores with a clear preferred orientation and an average long axis of 1.6 mm. We interpret this preferred orientation as an indication of the use of kiln drying while the clay was still too wet (Semiz and Duman, 2017). The matrix color of the samples in this group, as examined under polarized light, is usually reddish.

Subgroup 1a: The 5 samples from the Höyük settlement contain less rock fragments and more abundant carbonates, as compared to other examples in group 1. Samples E25 and E26 each have a few small quartz grains, with small amounts of pyroxene minerals, and abundant carbonates. Samples E27 and E28 consist of abundant pyroxene and plagioclase minerals, carbonates, and quartzite gravels. In particular, sample E27 contains abundant amounts of carbonate and quartzite gravels, as well as large pyroxene, plagioclase, and muscovite minerals (Fig. 3b). Sample E29 contains distinct carbonate content and evidence for oxidation in its small cracks. Sample E30 from Asmakuyu settlement has abundant pores and dominant amounts of muscovite.

Group 2: The 20 sherds in this group have medium abundant rock fragments, composed mostly of quartzite, with less carbonate minerals, mica schist, or muscovite-quartz schists. The dimensions of the rock fragments are relatively small, with average lengths of 0.25 mm. Additionally, we observed larger amounts of quartz, larger sizes of pyroxene, and larger plagioclase and biotite minerals than in the other groups. The overall percentages of quartz, pyroxene, and plagioclase are higher than in the other groups. Quartz minerals have lengths of up to 0.75 mm and pyroxene minerals have lengths up to 0.25 mm. The plagioclases are characterized by distinct polysynthetic twinning (Fig. 3c). Sample E36 from Beycesultan contains some fragments of the amphibole mineral. We also observed carbonate minerals (especially monocrystalline calcite) in the samples in this group, though quantities were not as high as in the first group. The percentage of pores is also relatively low, though some samples of this group show preferred orientation of the pores, with a long axis dimension up to 0.5 mm. Sample E17 from the Çeşmebaşı settlement had some unique features. It is composed of abundant quartz, large plagioclase, pyroxene and metamorphic rock fragments. Sample E22 from Göceler Höyük also differed from the other samples in this group due to its abundant quantity of carbonate, together with quartz and quartzite gravels (Fig. 3d). Samples E23 and E24 from Göceler Höyük have smaller rock fragments (lengths of 0.5-1mm), generally composed of quartzite and muscovite-quartz schists. These samples also have smaller pyroxene and plagioclase minerals, and a relatively high carbonate content. Samples E31 and E32 from Asmakuyu settlement include abundant quartz, plagioclase, pyroxene, and carbonate, and an unoxidized dark grey core.
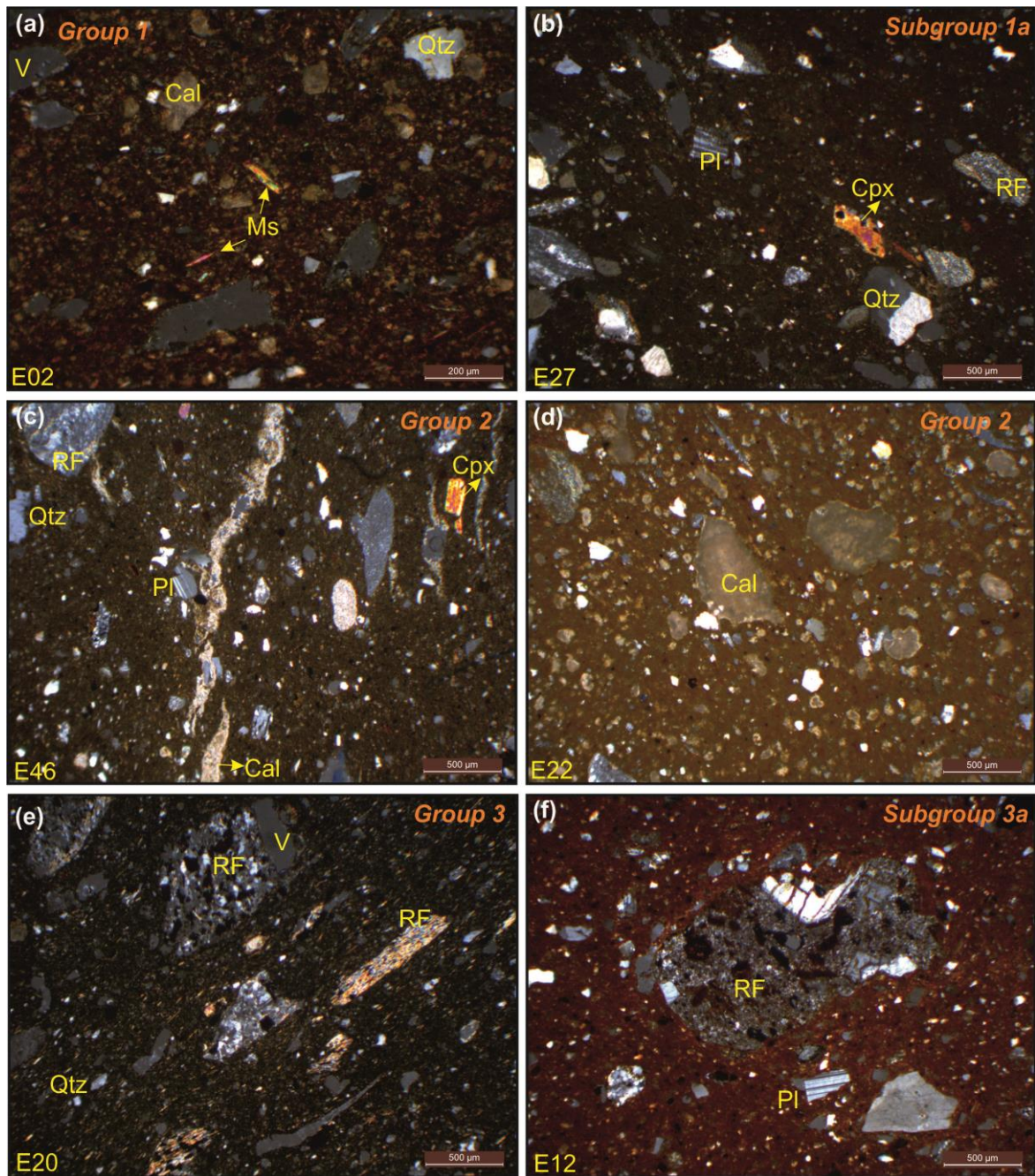
Figure 3 Photomicrographs (Transmitted light, crossed polarization) of select ceramic samples (Qtz:Quartz, Pl:Plagioclase, Cal:Calcite, Cpx:Pyroxene, Ms:Muscovite, RF: Rock fragments) (abbreviations from Kretz 1983).

Group 3: This group of 18 sherds is characterized by dominant large-grained (up to 3mm in length) metamorphic rock fragments (MRF), composed of quartzite, mica schist, and quartz-mica schists. The dimensions of the rock fragments are relatively large, with average lengths of 3.0 mm. These samples also contain large quantities of limestone fragments, with lengths up to 3.5 mm. Samples E09 and E11 from Kocakaya settlement contain the largest quantity of rock fragments in this group and they have calcite minerals with polysynthetic twinning (Fig. 3e). Samples E13, E14, E15, and E16, E18 come from Belkuyu Höyük and the Çeşmebaşı settlement,

respectively. They all contain smaller rock fragments, with abundant quartz and muscovite minerals. The quartz minerals are generally angular with a long axis between 0.6-1.5 mm. less abundant pyroxenes and plagioclase minerals, as well as other opaque minerals have smaller dimensions. Sample E16 has distinct thin and long pores, with a long axis of up to 0.8 mm. Preferred orientation of these pores indicates the ceramic clay was kiln-dried too early in the production process (Semiz and Duman, 2017). On the other hand, samples E33 and E34 from Kocainüstü settlement are characterized by their complex internal structures, which contains clay pellets

and large amounts of rock fragments. These dark greyish color samples from Kocainüstü Tepe also contain large quartz minerals and abundant quartzite gravels. Samples E41 and E42 from Beycesultan are characterized by large and abundant rock fragments as well as their quartz components. The rock fragments consist of rounded grains and quartzite sands of almost 1 mm in length, as well as carbonate minerals.

Subgroup 3a: Sample E10 from Kocakaya settlement is a unique ceramic, with abundant fragments of volcanic rocks (dacite), as well as plagioclase and mica minerals. Sample E12 from Ilıman Hoyuk has larger pyroxene and plagioclase crystals (with zoning), volcanic rock fragments, and quartzite gravels (Fig. 3f). The components of these two samples show significant differences from the dominant lithologic structure of the region.

5.2. XRD analyses

Fig. 4 shows the XRD patterns for a selection of samples from each of the three petrographic groups. Sample E05 of group 1 from Beycesultan has distinct quartz, feldspar, pyroxene, calcite, and illite/muscovite spikes, representing the group's relatively high calcite content, also observed in the petrography. In sample E27 of subgroup 1a, only the illite/muscovite could not be identified (Fig. 4a), perhaps related to a higher firing temperature than the other samples.

The samples from group 2 have similar mineralogical compounds, including quartz, feldspar, and calcite, with relatively small amounts of pyroxene and illite/muscovite. E24 sample from Göceler Hoyuk could not be identified to illite/muscovite minerals. Samples E32 from Asmakuyu Tepe settlement and E36 from Beycesultan contain more pyroxene and feldspar minerals than the other sample in the group.

In group 3, samples E08 and E34 have significant quartz, illite/muscovite, and calcite quantities, while lacking feldspar and pyroxene. Samples E15 and E18 from Belkuyu Höyük and the Çeşmebaşı Settlement have dominant quartz and feldspar but lack illite/muscovite. XRD detected differences with the samples from the mountainous settlements such as sample E15 from Belkuyu Höyük, where feldspar content was higher than in sample E18 from the Çeşmebaşı Settlement.
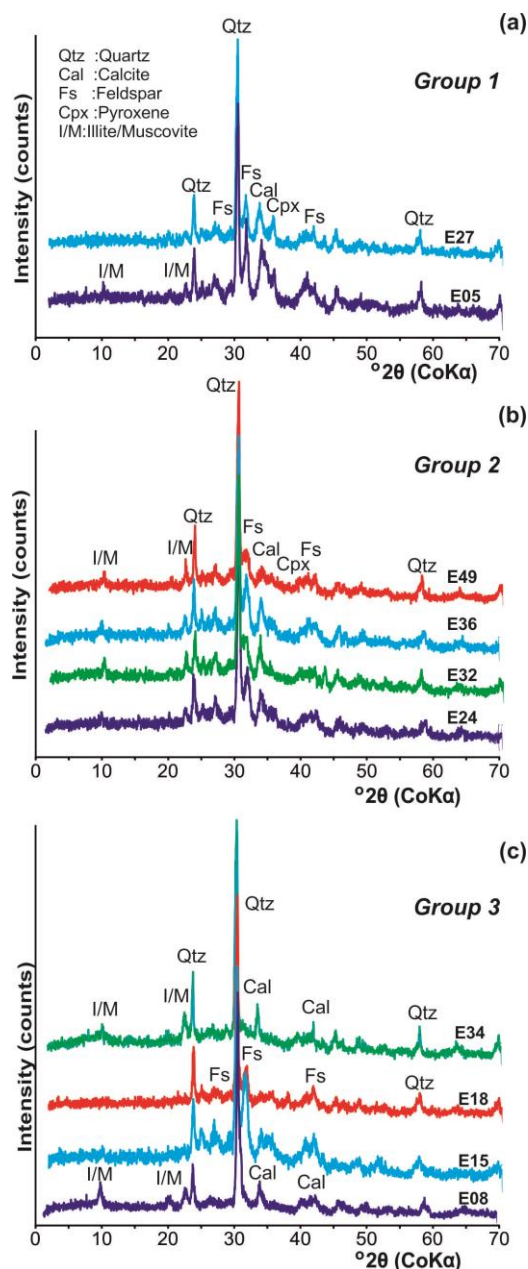
Figure 4 X-Ray powder diffraction patterns of the ceramic sample groups

5.3. Geochemical Results

Our XRF analysis recorded the main and trace elements from 21 ceramic samples in order to identify the compositional differences between the petrographic groups (Table 2). We evaluated the element quantities using paired correlation (Figs. 6-9) and triangular classification diagrams (Fig. 5). Paired correlation diagrams, also called binary diagrams, help to illuminate compositional differences among samples. The analysis supported by these diagrams demonstrated that the chemical contents of the samples also divide into 3 groups that reflect the differences seen in the petrographic analysis.

Table 2. Chemical analyses of the representative ceramic samples.

Groups		Group 1				1a	Group 2								Group 3							3a
Settlements		BYH			ATS	HS	GH		ATS		BYH				KS			ÇS	BH	KTS		KS
Element	Unit	E01	E02	E05	E30	E27	E23	E24	E31	E32	E36	E43	E46	E49	E08	E09	E11	E18	E15	E33	E34	E10
SiO_2	%	57.90	52.04	50.28	51.97	54.94	56.43	56.89	59.93	58.59	57.30	59.96	55.97	58.59	56.53	60.12	60.70	60.36	55.74	59.76	58.67	57.63
TiO_2	%	0.69	0.76	0.79	0.92	0.85	0.95	0.96	0.93	0.95	0.94	0.91	0.92	0.95	1.19	1.03	1.05	1.09	1.01	1.08	1.02	0.97
Al_2O_3	%	12.02	14.55	15.88	14.10	14.83	18.95	18.05	17.10	17.07	17.28	17.00	17.46	17.25	21.72	18.67	18.48	18.85	21.19	16.65	19.02	19.65
Fe_2O_3	%	5.67	6.91	6.05	9.23	6.31	7.73	7.02	6.61	6.32	6.42	6.20	6.39	6.66	8.65	7.16	7.06	7.55	8.16	10.11	7.95	6.54
MnO	%	0.12	0.11	0.13	0.17	0.12	0.12	0.14	0.12	0.11	0.14	0.14	0.14	0.12	0.08	0.14	0.12	0.12	0.15	0.21	0.13	0.09
MgO	%	3.80	3.20	5.97	9.48	3.45	2.44	2.51	2.95	3.04	4.24	3.93	3.62	3.77	1.24	2.08	2.13	2.32	2.94	6.27	3.33	2.36
CaO	%	16.33	18.76	16.06	10.54	14.89	7.99	9.23	6.94	8.15	7.53	5.82	10.04	6.72	6.96	6.26	5.11	4.79	4.79	2.84	6.06	6.58
Na_2O	%	0.84	0.57	1.06	1.52	0.90	0.70	1.17	1.36	1.45	0.93	1.15	0.93	1.15	1.06	1.00	1.13	1.02	1.22	1.02	0.60	1.56
K_2O	%	2.33	2.56	3.39	1.73	3.28	4.43	3.62	3.71	3.72	4.35	4.28	4.05	4.25	2.12	3.13	3.76	3.54	4.29	1.64	2.53	4.28
P_2O_5	%	0.28	0.39	0.30	0.30	0.31	0.23	0.35	0.51	0.73	0.34	0.32	0.46	0.32	0.31	0.30	0.38	0.24	0.36	0.34	0.55	0.32
Total		99.98	99.85	99.9	99.97	99.89	99.95	99.92	99.88	99.85	99.9	99.99	99.98	99.78	99.86	99.89	99.92	99.87	99.85	99.93	99.84	99.98
Ba	ppm	632.0	1474.0	1399.0	910.0	1136.0	839.0	1232.0	1757.0	2628.0	1003.0	1120.0	1091.0	951.0	762.0	1569.0	1426.0	904.0	1139.0	1056.0	1012.0	1218.0
Rb	ppm	77.0	83.5	124.2	72.3	111.3	142.1	151.5	152.9	152.8	148.7	147.9	139.3	151.5	87.1	148.1	140.7	147.3	188.2	43.8	95.7	174.4
Sr	ppm	178.8	229.8	1197.0	188.4	458.3	252.4	395.1	426.0	522.5	557.8	575.3	481.8	505.5	180.1	355.3	435.2	299.0	289.0	96.6	130.8	563.7
Y	ppm	23.5	23.3	27.4	26.6	24.6	29.8	30.3	28.4	29.4	27.7	29.4	26.2	28.3	37.1	31.3	30.5	30.8	34.7	26.7	32.8	26.4
Zr	ppm	259.0	152.2	232.2	157.6	222.2	210.0	279.0	323.9	281.0	299.1	340.8	240.6	318.5	290.8	344.8	293.0	262.4	260.7	159.1	263.2	237.5
Nb	ppm	14.2	12.8	16.4	13.5	16.1	19.3	22.5	21.8	21.2	21.7	21.4	18.0	20.6	25.5	22.8	23.4	23.6	22.0	14.1	21.0	19.6
Th	ppm	12.8	13.8	18.8	11.6	16.9	20.7	25.9	24.5	27.9	22.7	23.1	19.4	24.0	18.7	25.4	26.6	23.7	29.2	9.7	26.0	25.2
Cr	ppm	592.1	340.6	96.6	417.6	129.8	118.1	119.5	124.3	111.2	99.5	117.1	104.8	120.6	108.4	118	86.3	136.4	135.8	515.6	308.1	90.8
Ni	ppm	360.2	370.7	76.2	355.8	133.5	129.7	113.8	92.5	79.0	97.6	99.8	89.8	117.3	57.3	106.9	89.2	149.1	104.9	267.7	209.8	88.2
V	ppm	82.5	125.1	112.3	171.4	111.5	135.0	138.0	131.5	189.6	136.7	125.3	130.8	133.7	166.8	145.4	122.0	147.2	183.2	202.0	202.0	120.1
Hf	ppm	9.2	7.6	7.6	8.9	7.6	6.7	6.9	9.6	8.8	9.0	11.5	7.3	11.2	7.3	9.3	9.4	10.7	10.3	3.6	8.2	11.3
Pb	ppm	25.4	29.1	27.5	17.6	22.5	30.6	37.9	35.9	43.5	36.6	37.8	32.4	36.8	24.1	40.0	41.8	33.1	44.4	16.3	36.5	35.0
Co	ppm	78.7	64.8	37.9	71.6	60.0	42.8	72.2	47.3	46.8	58.7	67.7	40.3	84.9	39.9	67.7	60.0	94.6	54.2	64.2	76.8	76.8
U	ppm	< 1,0	< 0,6	6.7	< 0,6	2.5	1.8	3.4	4.0	5.7	4.6	5.0	3.2	2.9	2.2	2.5	4.8	3.5	3.1	< 1,0	< 0,5	4.1
W	ppm	421.0	234.3	192.6	289.0	303.0	168.4	323.2	232.6	275.1	425.2	493.6	202.8	448.4	154.7	346.5	304.4	1130.0	220.4	139.8	172.2	398.3
Ga	ppm	11.9	14.1	18.9	15.4	17.1	23.1	21.9	20.2	19.2	21.6	20.6	20.4	21.1	24.6	22.1	22.1	25.4	30.2	15.4	19.5	25.4
Cu	ppm	17.7	22.6	34.2	43.6	32.1	38.6	36.8	36.2	37.2	33.3	31.8	34.2	33.8	22.5	39.5	40.2	43.6	44.7	46.6	34.2	34.2
Zn	ppm	67.9	86.3	79.2	108.6	73.3	103.5	91.6	93.7	88.7	75.0	71.5	90.1	94.4	75.1	92.8	106.3	89.6	130.2	88.2	98.5	94.0
Se	ppm	1.1	1.2	0.8	0.6	0.7	0.1	0.4	1.2	0.8	0.8	1.2	0.8	0.8	0.4	< 0,5	0.7	1.1	0.7	< 0,5	0.6	1.0
As	ppm	25.2	76.1	19.8	9.7	11.5	28.7	19.5	20.1	43.0	15.9	14.2	16.8	15.1	19.0	15.4	17.3	13.4	4.4	11.4	24.0	6.2
Nd	ppm	65.3	78.8	66.2	54.2	62.4	61.8	120.3	67.0	80.7	70.2	114.8	57.1	111.8	98.0	79.0	86.4	114.9	62.1	57.7	106.0	119.7
Cr/V		7.18	2.72	0.86	2.44	1.16	0.87	0.87	0.95	0.59	0.73	0.93	0.80	0.90	0.65	0.81	0.71	0.93	0.74	2.55	1.53	0.76
Y/Ni		0.07	0.06	0.36	0.07	0.18	0.23	0.27	0.31	0.37	0.28	0.29	0.29	0.24	0.65	0.29	0.34	0.21	0.33	0.10	0.16	0.30
CIA		38.13	39.93	43.64	50.57	43.75	59.09	56.28	59.32	56.70	56.62	59.54	53.74	58.75	68.17	64.24	64.89	66.84	67.31	75.17	67.43	61.30
ICV		2.48	2.26	2.11	2.38	2.01	1.29	1.37	1.31	1.37	1.45	1.34	1.49	1.37	0.98	1.11	1.10	1.08	1.06	1.39	1.14	1.14
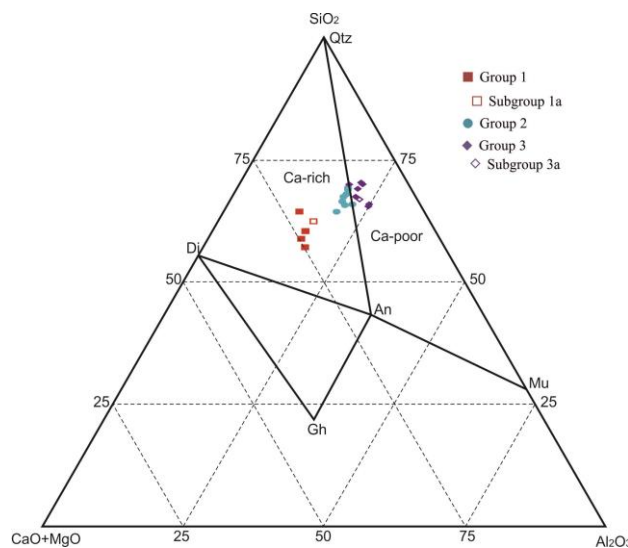
Figure 5 (CaO+MgO) – Al₂O₃ – SiO₂ (wt%) ternary diagram (Di = diopside; Gh = gehlenite; An = anorthite; Mu: mullite)

The main components of the samples are oxides that tend to be mobile and are impacted by various secondary effects such as liquid flow, decay, and diffusion. Pottery production itself can impact these oxides from the raw materials (Zimmermann et al., 2015). Although these oxide quantities are modified by all of these effects, researchers can still use them to delineate different ceramic recipes (Noll, 1978; Heiman, 1989). The SiO_2-(CaO+MgO)-Al_2O_3 triangular diagram displays clear differences between the three petrographic sample groups (Fig. 5). Groups 1 and 2 sit within the quartz-diopside-anorthite triangle, whereas group 3 sits within the quartz-anorthite-mullite triangle. Relative to the other two groups, the samples of group 3 have low levels of CaO and MgO and high levels of Al_2O_3. Thus, in terms of the main component oxides (SiO_2, Al_2O_3, Fe_2O_3, TiO_2, MgO, CaO, Na_2O, K_2O), the samples are clearly divided into three compositional groups that parallel the petrographic groups (Fig. 6). Group 1

samples have the lowest $SiO_2+Al_2O_3$ contents, whereas samples from groups 2 and 3 have similar $SiO_2+Al_2O_3$ contents to each other, but show differ-

ences in their $Fe_2O_3+TiO_2/CaO+MgO+Na_2O+K_2O$ contents.
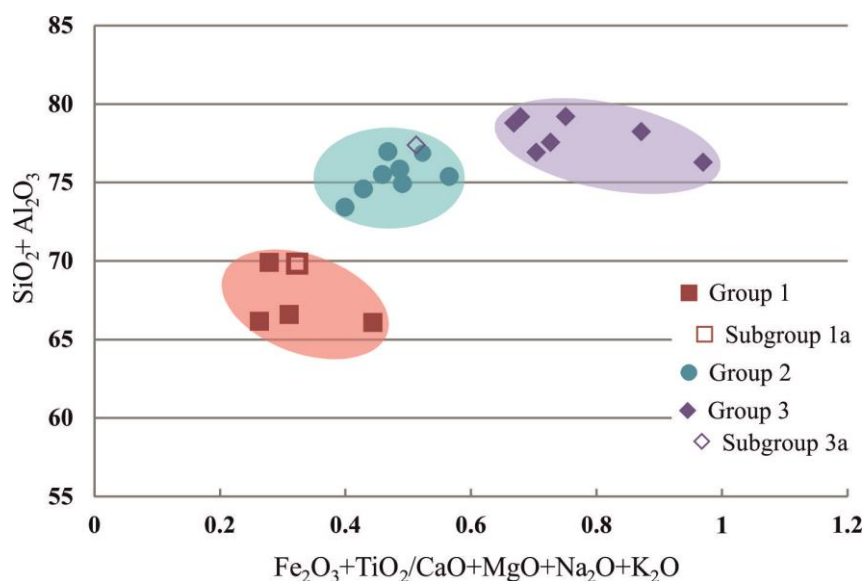
Figure 6 Binary diagram of SiO₂+Al₂O₃ versus Fe₂O₃+TiO₂/CaO+MgO+ Na₂O+K₂O (wt%) in select samples of the Upper Meander Basin.

The differences in the main component oxides seem to be directly related with the siliceous and carbonate mineral contents of the samples. In order to identify more specific compositional differences, we used paired correlation diagrams to evaluate the main component oxide contents (Figs. 7-8). We see clear differences in the CaO contents of the sample groups, with the highest CaO content in group 1, averaging 15.3%, and the lowest content in group 3, with group 2 in the middle with an average of 7.80% CaO (Fig. 7a). In our petrographic analysis, we had already detected abundant calcite minerals in groups 1 and 2. In terms of SiO_2 content, Group 1 has the lowest SiO_2 level, averaging 53.43%, whereas the SiO_2 content of the other two groups overlap, internally ranging between 56.4-60.7% (Fig. 7b). High levels of SiO_2 reflect the abundant quartz and/or quartzite contents in the samples. In terms of TiO_2, Group 3 has the highest levels, with Group 2 next, and Group 1 on average the lowest (Fig. 7c). In terms of K_2O+Na_2O, Group 2 has the highest average, while Group 1 is lower, but Group 3 spans both (Fig. 7d). The abundancies of these oxides relate to the

metamorphic rock fragments (mica schist and quartzite) found in the samples. Adding MgO into the analysis highlights how pyroxene minerals also accentuate the differences among the groups (Degryse and Poblome, 2008; Breakmans et al., 2011) (Fig. 7d).

A geochemical analysis of trace elements aids in the interpretation of the general composition of the raw geological materials used in the ceramics and helps trace the origin of these materials (McLennan et al., 1990). In particular, trace elements like Cr, Zr, and Ti can serve as geochemical pathfinders because of their relationship to special petrologic species (Mommsen, 2001; Belfiore et al., 2007; Iordanidis et al., 2009). Like the main elements, the trace elements can also reveal similarities and differences between the petrographic groups. Fig. 8 contains four CaO+MgO correlation diagrams to highlight relative quantities of the trace elements Sr, Y, Nb, and Ba/Th in the samples. The quantities of Nb, Y, and Ba/Th are low in all of the groups, and Sr is high in all of the groups, relating to the various mineralogical combinations.
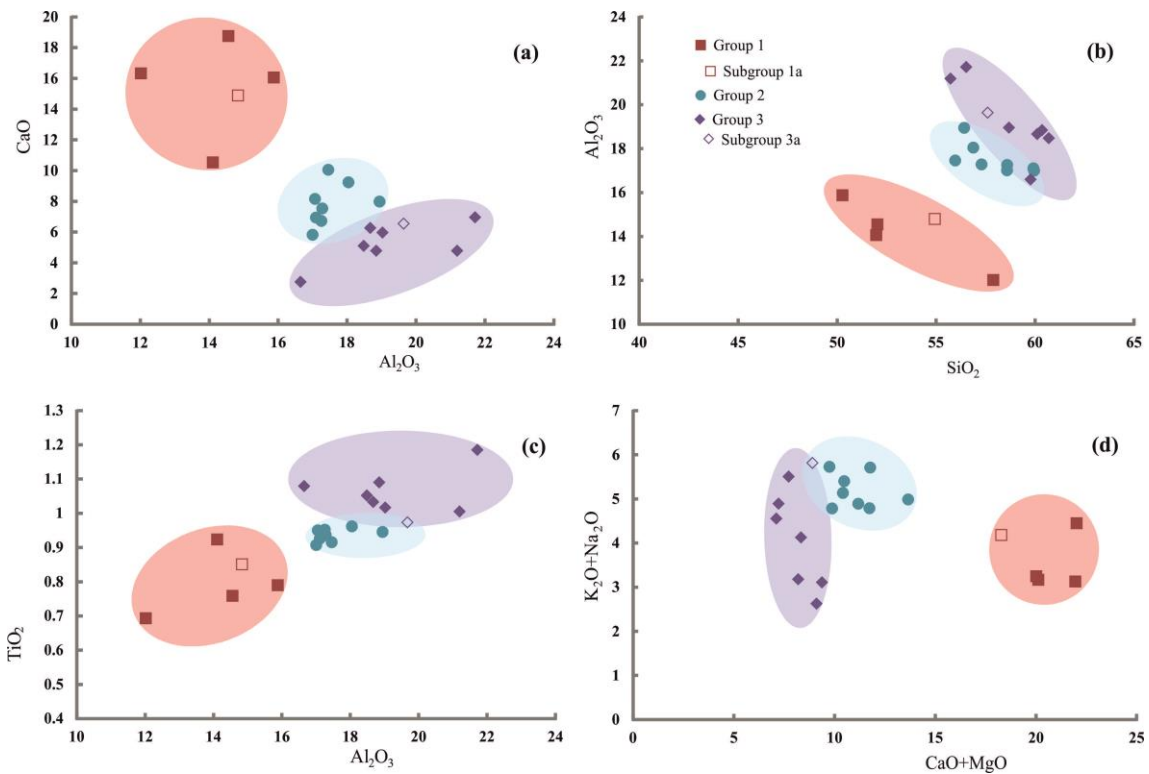
Figure 7 Relationships between (a) CaO and Al2O3 (b) Al2O3 and SiO2 (c) TiO2 and Al2O3 (d) K2O+Na2O and CaO+MgO in select samples of the Upper Meander Basin
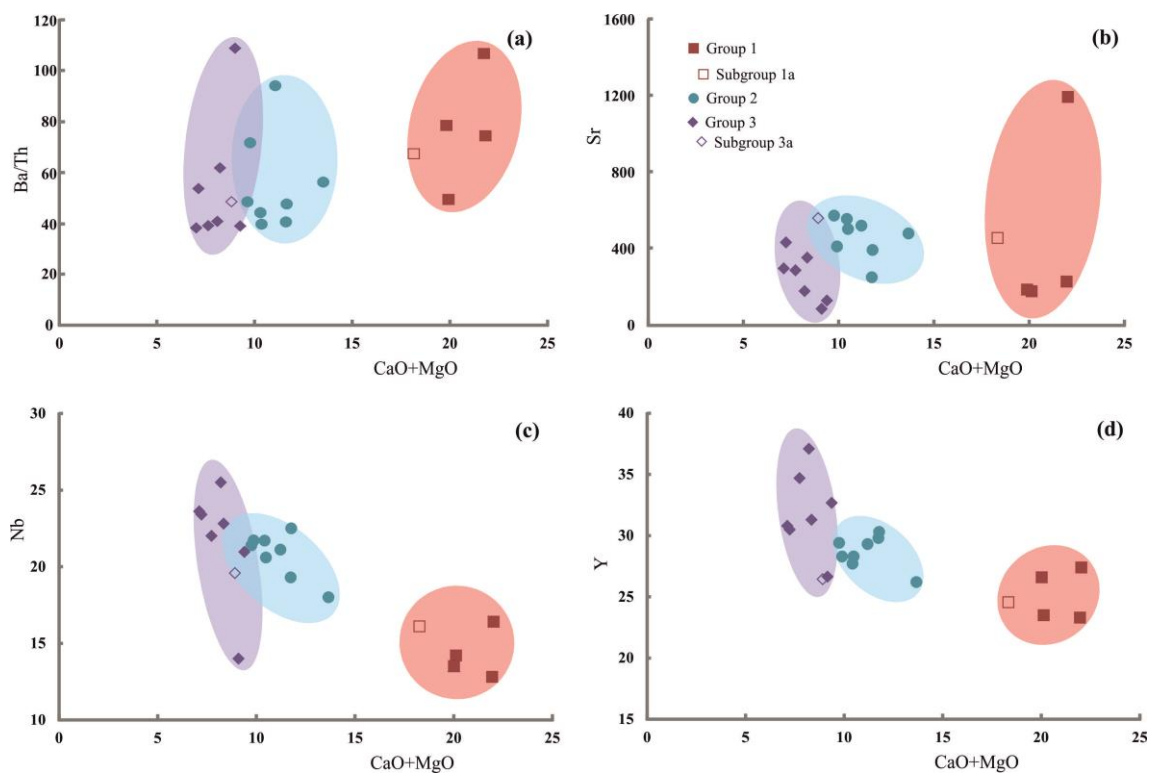
Figure 8 Relationships between (a) Ba/Th (b) Sr (c) Nb (d) Y and CaO+MgO (wt%) in select samples of the Upper Meander Basin.

6. DISCUSSION

6.1. Chronologies of the sample groups

The three overlapping petrographic and chemical groups, which consist of samples from various periods, provide useful information about diachronic production at mountainous, plateau, and lowland communities in the Upper Meander Basin. Group 1 is mainly composed of samples from the EBA II layers at Beycesultan Höyük and the MBA layers at the Höyük settlement. These two lowland sites have ceramics that are similar in terms of their mineralogical components. These mineralogic characteristics indicate the existence of metaclastics in the recharge area of the clay sources, and these sources cause Group 1 ceramics to differ significantly from the ceramics of Groups 2 and 3.

On the other hand, Group 1 ceramics show similarities with those of the MBA layers at the Höyük settlement in terms of their high carbonate (CaO) densities. High CaO is caused by limestone and/or marble rocks in the source area, which can be tied to the abundant calcite minerals in the samples. At Beycesultan Höyük, extra carbonate appears to have been added during the preparation process. This intentional addition was highest in the EBA, while decreasing in the MBA, which is possible even if the same clay deposits were used in both periods. The natural rocks of the Çivril plain appear to have high carbonate levels, reaffirming local production. Calcite-tempered pottery is also significantly more resistant to mechanical stress than grog-tempered pottery, and may be more resistant to thermal shock as well (Hoard et al., 1995). This may have led to heightened intentional use of carbonate minerals at the lowlands settlements. In contrast, samples from mountain-based settlements had lower levels of carbonate minerals, likely due to the abundant inclusion of metamorphic rock fragments instead.

The Group 2 samples are mostly MBA ceramics from Beycesultan Höyük, a lowlands settlement in the Basin. The characteristics of this Group are situated between those of Groups 1 and 3, but in general there are more similarities with Group 1. The Group 2 samples contain dense carbonate minerals, relating to the carbonated lithologies spread over a wide area of the Çivril plain. There are remarkable similarities between the Beycesultan material and the MBA samples from the plateau settlement of Göceler Höyük (E22, E23, E24). Overall, however, the Group 2 samples show enough differences in their mineralogical contents to indicate local production at different settlements, especially in the mountainous areas.

The Group 3 samples consist mostly of MBA ceramics from the mountainous parts of the Basin,

with diverse mineralogical compositions within this group. In general, rock inclusions are more prevalent in Group 3 than in Group 2. The subgroup 3a (Ilimanlı Höyük sample: E12 and Kocakaya sample: E10), differ from the basic Group 3 profile due to the dominance of volcanic rocks and quartzite gravels. This lithology is related to the porphyroid types of rocks within the Afyon zone on the northern part of the study area. Given the diversity of samples at Kocakaya, it would appear that the ceramics there come from two different clay deposits.

EBA II samples from the mountainous region have two different general structures. The Asmakuyu Tepe samples are similar to samples from both Groups 1 and 2, especially reflecting the extremely complex structure of Beycesultan ceramics with rough textures and grog temper. On the other hand, the Kocainüstü Tepe samples are closer to Group 3 samples. This variety of clay structure decreases over the course of the MBA, but differences between the samples from the two settlements are still observable at the end of this period. These differences in the samples from the different sites seem to reflect differences in clay sources fed by different source rock areas.

These archaeometric results indicate that the societies within the research area saw a level of specialization in pottery production during the EBA II. These results parallel what we observe in the other archaeological evidence. Although settlements in the mountain, plateau, and lowland areas used distinct clay deposits based on their local geological contexts, all areas used similar production technologies. Large settlements in the lowland of the Basin, which had seen continuity of habitation since the Late Chalcolithic Age, developed into significant central settlements during the EBA. These large settlements led a local three-tiered settlement hierarchy (Dedeoğlu, 2016). Beycesultan Höyük, at 15 hectares, was certainly a prominent center within the EBA settlement hierarchy. Excavation data from this site reflect contemporary complexity in social organization, with architectural differentiation, craft specialization, abundant status objects, and burial disparity all indicating an internal hierarchical structure in this society (Lloyd and Mellaart, 1965, Abay and Dedeoğlu, 2014). The Asmakuyu Tepe and Kocainüstü Tepe settlements, located in the mountainous area on the southwestern part of the plain containing Beycesultan Höyük, appear to be much smaller hilltop settlements that were likely part of a settlement and fortification system controlled from Beycesultan Höyük during the EBA II.

Archaeological data also indicate a well-organized political structure in the Basin during the MBA. This organization, which again developed around the

center at Beycesultan Höyük, seems to have controlled a broad area especially in the northern part of the Basin. The number and dimensions of settlements increased gradually over this period, reflecting a remarkable population increase in the Basin. The rising expertise in production also reflects this situation, particularly when compared with the EBA, in terms of ceramic recipes and kiln firing techniques.

6.2. Production Technologies

The presence and absence of particular mineral associations often provides clues for the estimation of ceramic firing temperatures (Iordanidis et al., 2009). The presence of quartz and feldspar minerals suggests a minimum firing temperature of about 900°C, with resistance up to 1000°C (Mirti and Davit, 2001). Quartz can be a component of the raw material derived from local natural clays or it can be added to clay as an inclusion. Calcite and illite/muscovite minerals also aid the estimation of firing temperatures. While calcite can be a primary component of natural clay, its presence in ceramics may also result from secondary percolation caused by sedimentation processes after burial (pore filling) (Cau et al., 2002; Semiz and Duman, 2017). Calcite survives in ceramics up to a temperature of about 600°C, subsequently being partially degraded until it is consumed completely at about 800-850°C. At temperatures over 800°C, free CaO reacts with free silica and aluminum derived from the degradation of clay minerals, thereby causing the formation of calcium silicates and alumina calc-silicates (such as gehlenite and pyroxene) (Iordanidis et al., 2009; Ortega et al., 2010). Illite/muscovite is exposed to degradation processes between 700-1000°C, with illite disappearing at 900°C and gehlenite appearing at 800-850°C (Cultrone et al., 2001; Hein et al., 2002).

The results of the XRD analyses indicate no significant differences between the firing temperatures of the three ceramic groups. We interpret the widespread peaks of illite/muscovite and calcite as indicating relatively low firing temperatures (<800°C) (Iordanidis et al., 2009; Kramar et al., 2012). We also read the presence of calcite minerals crystalized in thin sections as primary calcites. The lack of illite/muscovite peaks in some Group 3 samples indicates that their firing temperature may be a little higher than the other samples. We conclude from these observations that the EBA II fortified settlements of Kocainüstü Tepe and Asmakuyu Tepe, located in the mountainous areas, shared technological practices with the central site of Beycesultan Höyük. Although ceramics in the mountains and the lowlands were produced in similar ways, the differences in chemical and mineralogical contents of the sherds

from EBA II Beycesultan Höyük reaffirm that ceramics were separately produced in the two areas with different, local raw materials.

6.3. Sources of the inclusions

Fine texture clay comprises the main structure of the ceramic samples, and petrography is limited in its ability to analyze the geological sources at this scale. Temper added to the ceramics, on the other hand, is large enough to be characterized with this method. We can use petrography to begin to trace the origins of the rock fragments and minerals added as inclusions during the ceramic production process. In particular, feldspar and muscovite minerals provide significant data on the source area of the ceramics (Kibaroğlu, 2005). Within this framework, we interpret the sources of the inclusions included in the ceramic samples through an analysis of the metamorphic rock fragments, calcite, quartz, feldspar, pyroxene, and muscovite minerals.

Quartz, feldspar, and muscovite are the typical mineral components of granodiorite and metamorphic rocks. The high MgO, Cr and Ni contents of samples can additionally reflect the presence of mafic and ultramafic minerals in the source area. Coherent trace elements like Cr and Ni (Cr: 130-592 ppm; Ni: 133-370 ppm) are relatively high in the samples from Group 1 and moderate in some samples (E33 and E34) from Group 3 (Figs. 9a and b). Cr/Th and Cr/V rates are a good indicator of mafic-ultramafic compounds or dominant mafic-ultramafic components within clastic materials (Zimmermann et al., 2015), and Cr/V rates above 8% indicate mafic-ultramafic combinations of ophiolites. The rock inclusions in samples from Group 1 likely have an enrichment in ferromagnesian minerals, as observed in high Ni rates with depleted V (McLennan et al., 1993; Zimmermann et al., 2015). As seen in the Cr/V-Y/Ni diagram, Cr/V rates are <0.9% for samples from Group 2, between 1.2-7.2% for samples in Group 1, and between 1.5-2.5% for some samples in Group 3 (Fig. 9c). These rates are generally a lot lower than the values identified for primary basalts and ultramafic rocks (Zimmermann et al., 2015). The redundancy in Cr and Ni elements and the lack of redundancy in MgO, Cr/V and Cr/Th values indicates the possibility of few mafic and ultramafic minerals in the source areas.

We investigated possible causes for an enrichment of only the elements Cr and Ni. Green micas are generally chromium-plated muscovites, and their unique green color stems from the concentration of chrome and iron in these micas. Green mica (fustit or chromium plated muscovites) is common in metasedimentary rocks, especially in quartzites (Randive et al., 2005). The formation of green mica

quartzites has two different origins, starting with hydrothermal alteration. In this process, mica results either from the replacement of pre-existing rock or from hydrothermal solutions spread by magmatic intrusion. The second origin for green mica quartzites is the metamorphism of chrome-rich minerals within the source rock (Randive et al., 2005). Metaclastics are conventional in the western part of the Baklan Basin, and the abundant metaclastics in the ceramic samples from Group 1 and a selection of Group 3 samples support this relationship.
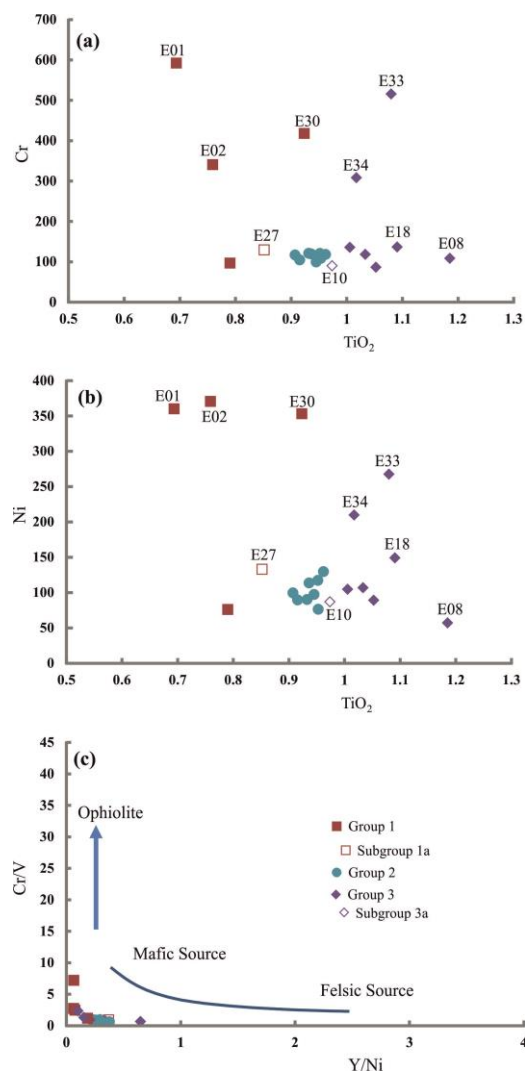
Figure 9 Relationships between (a) Cr and TiO₂ (b) Ni and TiO₂ (c) Cr/V and Y/Ni in select samples of the Upper Meander Basin

6.4. Raw Material Provenance

Geologists use the Chemical Index of Alteration (CIA) (Nesbitt and Young, 1982) and the Index of Compositional Variance (ICV) (Cox et al., 1995) to estimate alteration and/or degradation of source rocks. Several recent studies have applied these indices to the study of archaeological ceramic samples, following standard methods (Kibaroğlu, 2005;

Kibaroğlu et al., 2008; Hoeck et al., 2009; Jumbam et al., 2013; Diskin and Ashley, 2016). CIA is calculated from the quantities of various minerals (CIA= $[Al_2O_3/(Al_2O_3 + CaO + Na_2O + K_2O)]$ x 100). For example, unaltered magmatic and metamorphic rocks would have a CIA less than 50, whereas pure kaolins would be under 100. High CIA values indicate the alteration of a source rock, but sedimentary rocks also have high CIA values. The re-alteration of sedimentary rocks increases the clay mineral component of re-deposited or newly deposited sediments, thereby increasing Al_2O_3 (>20%) content and CIA values indirectly (Kibaroğlu, 2005). High levels of Al_2O_3 result from high levels of clay mineral content, also indicating strong alteration of the source rock. The average CIA values for our ceramic samples are 43.2 for Group 1; 57.5 for Group 2; and 66.9 for Group 3. These values show little and/or very little degradation effect in Groups 1 and 2, while Group 3 exhibits medium chemical degradation. The average CIA value of all the groups is lower than the average for shale (Post-Archean Australian Shale-PAAS: 70-75). Similarly, when Al_2O_3 values are considered as a proxy for clay mineral content, the average content is 14.3 for Group 1; 17.5 for Group 2; and 19.3 for Group 3. These low Al_2O_3 levels are interpreted as a lack of re-alteration of sedimentary rocks in the source area. These levels track the low CIA values, where the lowest levels are found in Group 1, while the highest are in Group 3.

ICV is calculated from the quantities of certain minerals ($Fe_2O_3+K_2O+Na_2O+CaO+MgO+MnO+TiO_2$)/ Al_2O_3), with results ranging from 0.01 in clay minerals to 1000 in silicates without clay (Hoeck et al., 2009). In our samples, ICV values have an average of 2.3 for Group 1; 1.4 for Group 2; and 1.1 for Group 3. These values are interpreted as reflecting small additions of extra minerals into the clay, the minerals also observed in the thin sections, namely muscovite, feldspar and/or pyroxene. The three groups lack significant differences in the measurement of ICV.

Together, the measurements for CIA, ICV and Al_2O_3 indicate a potential origin for the source rocks of the clay raw materials. The matrixs of the samples seem to be produced from sedimentary rocks, while the inclusions are rock fragments derived from metamorphic or geochemically equivalent rocks. We believe that the raw materials were gathered from a minimum of 2 and a maximum of 3 different clay deposits, each recharged by different fields. The samples of Group 1 include smaller amounts of clay minerals and more inclusions, but the overall trend in all groups is an increase in clay content in the MBA.

7. CONCLUSIONS

Our analyses investigated 49 ceramic samples from 11 prehistoric settlements located in the Upper Meander Basin in order to examine ceramic provenance and technology. We found a close relationship between the geological structure of the topography, settlement locations, and the mineralogic characteristics of the local ceramic products. High levels of Cr and Ni in the samples indicate that neither mafic nor ultramafic rocks existed in the source areas of the ceramics.

A comparison of the three ceramic groups indicates that a heat level of 800 ºC was not exceeded during the firing process. Firing appears more controlled during the MBA. Our evaluation of both the local geological profile and the mineralogy of the thin sections indicates that the ceramics at all settlements were local products.

We also note that regardless of settlement hierarchy patterns, ceramic production technologies were shared by all settlements, from Beycesultan Höyük to the surrounding hilltop settlements. We conclude that there was significant information transfer during the EBA II and MBA in this region, perhaps resulting from a high level of system integration. Although they shared methods of producing the ceramics, all of the settlements used local raw material sources. Thus, each settlement independently produced their own ceramics. The results of our archeometric analyses of ceramic samples from the Upper Meander Basin have confirmed previous archaeological inferences based on macroscopic data.

ACKNOWLEDGEMENTS

REFERENCES

Abay, E. (2008) Die Neolithischen Fundorte in Der Çivrilebene im Oberen Maandegebiet. Erste Ergebnisse Einer Gelendebegehung." in Bonatz, D.; R. M. Czichon und F.J. Kreppner, eds., Fundstellen, Gesammelte Schriften zur Archaeologie und Geschichte Altvorderasien, ad honorem Hartmut Kühne. Wiesbaden: Harrassowitz Verlag, pp. 1-8.

Abay, E. and Dedeoğlu, F. (2009) Preliminary Report of Beycesultan 2007-2008 Excavation Campaigns. Arkeoloji Dergisi 13, pp. 53-79. (In Turkish)

Abay, E., and Dedeoğlu, F. (2014) Beycesultan Höyük Excavation Project: New Archaeological Evidence from Late Bronze Age Layers. Arkeoloji Dergisi, 17, pp. 1-39. (In Turkish)

Altay, T. and Dumlupınar, İ. (2013) Dinar (Afyon)-Baklan (Denizli) Kömür Havzalarında Bulunan Killerin Jeolojik ve Mineralojik İncelenmesi (Geologic and Mineralogic investigsations on clays from coal deposits in Dinar (Afyon)-Baklan (Denizli) region, western Turkey). AKU Journal of Science and engineering, Vol. 13, pp. 1-10. (In Turkish)

Akkiraz, M.S., Akgün, F., Örçen, S., Bruch, A.A. and Mosbrugger, V. (2006) Stratigraphic and palaeoenvironmental significance of Eocene microfossils from the Başçeşme formation, Denizli province, Southwest Anatolia. Turkish Journal of Earth Sciences, Vol. 15, pp. 155-180.

Ay, A.M, Aytar, N. and Tolluoğlu, A.Ü. (1999) Orta Kambriyen yaşlı Sandıklı porfiroyidi'nin petrografik ve jeokimyasal karakteristikleri (The characteristics of petrographical and geochemical features of Middle Cambrian aged Sandıklı Porphiroids). 52nd Geological Congress of Turkey, pp. 263-270. (In Turkish)

Belfiore, C.M., Day, P.M., Hein, A., Kılıkoglou, V., La Rosa, V., Mazzoleni, P. and Pezzino. A. (2007) Petrographic and chemical characterization of pottery production of the Late Minoan I kiln at Haghia Triada, Crete. Archaeometry, Vol. 49, No.4, pp. 621-653.

Braekmans, D., Degryse, P., Poblome, J., Neyt, B., Vyncke, K. and Waelkens, M. (2011) Understanding ceramic variability: an archaeometrical interpretation of the Classical and Hellenistic ceramics at Düzen Tepe and Sagalassos (Southwest Turkey). Journal of Archaeological Science, Vol. 38, pp. 2101-2115.

Brunelli D., Levi, S.T., Fragnoli, P., Renzulli, A., Santi, P., Paganelli, E. and Martinelli, M.C. (2013) Bronze Age Pottery from the Aeolian Islands: Definition of Temper Compositional Reference Units by an integrated mineralogical and microchemical approach. Apllied Physics A, Vol. 113, No. 4, 855-863.

Carvajal López, J.C. and Day, P.M. (2015) The production and distribution of cooking pots in two towns of South East Spain in the 6th-11th centuries. Journal of Archaeological Science: Reports, Vol. 2, pp. 282-290.

Cau, O.M.A., Day, P.M. and Montana, G. (2002) Secondary calcite in archaeological ceramics: evaluation of alteration and contamination processes by thin section study." in V. Kilikoglou, A. Hein, Y. Maniatis, eds,. Modern trends in scientific studies on ancient ceramics: papers presented at the 5th European Meeting on Ancient Ceramics, Athens 1999. BAR International Series, Vol. 1011, pp. 9-18.

Ceylan, M.A. (1998) Baklan-Çivril Havzası ve Yakın Çevresinin Hidrojeo-morfolojik Etüdü (Hydrogeomorphological survey of Baklan-Çivril Basin and surrounding area). PhD thesis, Marmara University. (In Turkish)

Cox, R., Low, D.R. and Cullers, R.L. (1995) The influence of sediment recycling and basement composition on evolution of mudrock chemistry in the southwestern United states. Geochimica et Cosmochimica Acta, Vol. 59, No. 14, pp. 2919-2940.

Cultrone, G., Rodriguez-Navarro, C., Sebastian, E., Cazalla, O. and De La Torre, M.J. (2001) Carbonate and silicate phase reactions during ceramic firing. European Journal of Mineralogy, Vol. 13, pp. 621-634.

Day, M.P., Doumas, C.G., Erkanal, H., Kılıkoglou, V., Kouka, O., Relaki, M. and Şahoğlu, V. (2009) New Light on the "Kastri Group" A Petrographic and Chemical Investigation of Ceramics from Liman Tepe and Bakla Tepe, 24. Arkeometri Sonuçları Toplantısı, pp. 335-346.

Dedeoğlu, F. (2013) Regional Settlement Analysis in Upper Meander Basin: The Process of socio-economic change and transformation in organization of Early Bronze Age Sites. in Ö. Çevik, B. Erdoğu eds., Tematik Arkeoloji Serisi 1, Yerleşim Sistemleri ve Mekan Analizi, İstanbul: Ege Yayınları, pp. 20-42.

Dedeoğlu, F. (2016) A study on chalices from Beycesultan: Their function, social meaning and cultural interactions. *Mediterranean Archaeology and Archaeometry*, Vol. 16, No 2, pp. 13-32

Dedeoğlu, F., Ozan, A. and Konakçı, E. (2016) Yukarı Menderes Havzası Dağlık Kesim Yüzey Araştırması Projesi 2014 Yılı Çalışmaları (Upper Meander basin mountainous survey project). Research result meeting, Vol. 33, No. 2, pp. 553-563. (In Turkish)

Degryse, P. and Poblome, J. (2008) Clays for mass production of table and common wares, amphora and architectural ceramics at Sagalassos. in P. Degryse, and M. Waelkens, eds., Sagalassos VI. Geo- and Bio-Archaeology at Sagalassos and in Its Territory. Leuven: Universitaire Pers Leuven, pp. 231-254.

Dickinson, W.R. and Shutler, R. (2000) Implications of Petrographic Temper Analysis for Oceanian Prehistory. Journal of World Prehistory, Vol. 14, No. 3, pp. 203-266.

Diskin, S. and Ashley, C. (2016) Characterisation of archaeological ceramics from the Khwebe Hills of northern Botswana. Journal of Archaeological Science: Reports, Vol. 6, pp. 574-583.

Dora, O.Ö., Candan, O., Kaya, O., Koralay, E. and Dürr, S. (2001) Revision of 'Leptite Gneisses' in the Menderes masif: a supracrustal metasedimentary origin. International Journal of Earth Sciences, Vol. 89, No. 4, pp. 836-851.

Graciansky, P.Ch. (1972) Recherches géologiques dans le Taurus Lycien occidental." PhD diss., d'Etat, Université Paris-Sud.

Hawkins, J.D. (1998) Tarkasnawa King of Mira, 'Tarkondemos', Boğazköy Sealings and Karabel. Anatolian Studies, Vol. 48, pp. 1-31.

Heimann, R.B. (1989) Assessing the technology of ancient pottery: the use of ceramic phase diagrams. Archeomaterials, Vol. 3, No. 2, pp. 123-48.

Hein, A., Tsolakidou, A. and Mommsen, H. (2002) Mycenaean pottery from the Argolid and Achaia-a mineralogical approach where chemistry leaves unanswered questions. Archaeometry, Vol. 44, No. 2, pp. 177-86.

Hoard, R.J, O'Brien, M.J., Khorasgany, M.G. and Gopalaratnam, V.S. (1995) A materials-science approach to understanding limestone-tempered pottery from the Midwestern Unites States. Journal of Archaelogical Science, Vol. 22, pp. 823-832.

Hoeck, V., Ionescu, C., Ghergari, L. and Precup. C. (2009) Towards mineralogical and geochemical reference groups for some Bronze Age ceramics from Transylvania (Romania). Geologia, Vol. 54, No. 2, pp. 41-51.

Javanshah, Z. (2018) Chemical and mineralogical analysis for provenaning of the Bronze Age pottery from Shahr-i-Sokhta, South Eastern Iran. *SCIENTIFIC CULTURE*, Vol. 4, No 1, pp. 83-92.

Iordanidis, A., Garcia-Guinea, J. and Karamitrou-Mentessidi, G. (2009) Analytical study of ancient pottery from the archaeological site of Aiani, northern Greece. Materials Characterization, Vol. 60, pp. 292–302.

Jumbam, N.D., Georges-Ivo Ekosse, E. and Steele, J. (2013) Chemical characterisation of argillaceous sediments used for traditional pottery around Port St Johns, Eastern Cape Province, South Africa. Transactions of the Royal Society of South Africa, Vol. 68, No. 3, pp. 147-153.

Kibaroğlu, M. (2005) Sedimentary geochemical approach to the Provenance of the non-calciferous north Mesopotamian metallic ware. Archeometriai Műhely, Vol. 2, pp. 48-51.

Kibaroğlu M. and Hartmann, G. (2015) Application of SR-Isotope Geochemistry to Provenance Study of Archaeological Ceramics: A Case Study on the North Mesopotamian Metallic Ware from N-E Syria and SE Anatolia. Archaometrie und Denkmalpflege, Metalle Sonderheft, Vol. 7, pp. 104-106.

Kibaroğlu M., Falb, C. and Satır, M. (2008) On the Origin of the Northmesopotamian Metallic Ware A New View from Sediment Geochemistry." in Ü. Yalçın, eds., Anatolian Metal IV. Der Anschnitt, Beiheft, Vol. 21, pp. 211-223.

Kibaroğlu M., Sagona A., and Satir, M. (2011) Petrographic and geochemical investigations of the late prehistoric ceramics from Sos Höyük, Erzurum (Eastern Anatolia). Journal of Archaeological Science, Vol. 38, pp. 3072-3084.

Kilic, N.C, Kilic, S, Akgul, C.H (2017) An archaeometric study of provenance and firing technology of Halaf pottery from Tilkitepe (Eastern Turkey). Mediterranean Archaeology and Archaeometry, Vol. 17, No 2, pp. 35-48.

Konak, N. (2002) Türkiye Jeoloji Haritası (Geological maps of Turkey), 1: 500 000. Ankara: MTA publications. (In Turkish)

Konak, N., Akdeniz, N. and Çakır, H. (1986) Çal-Çivril Karahallı Dolayının Jeolojisi (Geology of the Çal-Çivril-Karahallı region). MTA Report No: 8945. (In Turkish)

Kramar, S., Lux, J., Mladenovic, A., Pritacz, H., Mirtic, B., Sagadin, M. and Rogan-Smuc, N. (2012) Mineralogical and geochemical characteristics of Roman pottery from an archaeological site near Mošnje (Slovenia). Applied Clay Science, Vol. 57, pp. 39-48.

Lloyd, S. (1972) Beycesultan Vol III, part 1, Late Bronze Age Architecture. The British Institute of Archaeology at Ankara, London.

Lloyd, S. and Mellaart, J. (1962) Beycesultan vol 1, The Chalcolithic and Early Bronze Age Levels. The British Institute of Archaeology at Ankara, London.

Lloyd, S. and Mellaart, J. (1965) Beycesultan vol 2, Middle Bronze Age Architecture and Pottery. The British Institute of Archaeology at Ankara, London.

Luke C., Roosevelt, C.H., Cobb, P.J. and Çilingiroğlu, Ç. (2015) Composing Communities: Chalcolithic through Iron Age survey ceramics in the Marmara Lake Basin, western Turkey, Journal of Field Archaeology, Vol. 40, No. 4, pp. 428-449.

Maritan, L., Nodari, L., Mazzoli, C., Milano, A. and Russo, U. (2006) Influence of firing conditions on ceramic products: Experimental study on clay rich in organic matter. Applied Clay Science, Vol. 31, pp. 1-15.

Mellaart, J. and Murray, A. (1995) Beycesultan Vol. III Part II: Late Bronze Age and Phrygian Pottery and Middle and Late Bronze Age Small Objects, The British Institute of Archaeology at Ankara, London.

McLennan S.M., Taylor, S.R., McCulloch, M.T. and Maynard, J.B. (1990) Geochemical and Nd-Sr isotopic composition of deep-sea turbidites: crustal evolution and plate tectonic associations. Geochimica et Cosmochimica Acta, Vol. 54, pp. 2015-2050.

McLennan, S., Hemming, S., McDaniel, D. and Hanson, G. (1993) Geochemical approaches to sedimentation, provenance, and tectonics." In M.J. Johnsson, A. Basu, eds., Geological Society of America Special Papers, Vol. 284, pp. 21-40.

Mirti, P. and Davit, P. (2001) Technological characterization of campanian pottery of type A, B and C and of regional products from ancient Calabria (Southern Italy). Archaeometry, Vol. 43, No. 1, pp. 19-33.

Mommsen, H. (2001) Provenance determination of pottery by trace elements analysis: problems, solutions and applications. Journal of Radioanalytical Nuclear Chemistry, Vol. 247, No.3, pp. 657-662.

Nesbitt, H. and Young, G. (1982) Early Proterozoic climates and plate motions inferred from major element chemistry of lutites. Nature, Vol. 299, pp. 715-717.

Nodari, L., Maritan, L., Mazzoli, C. and Russo, U. (2004) Sandwich structures in the Etruscan-Padan type pottery. Applied Clay Science, Vol. 27, pp. 119-128.

Noll, W. (1978) Material and techniques of the Minoan ceramics of Thera and Crete. in C. Doumas, H.C. Puchelt, eds., Thera and the Aegean World I, London, pp. 493-505.

Ortega, L.A., Zuluaga, M.C., Alonso-Olazabal, A., Murelaga, X. and Alday, A. (2010) Petrographic and geo-chemical evidence for long-standing supply of raw materials in Neolithic pottery (Mendandia site, Spain). Archaeometry, Vol. 52, No.6, pp. 987-1001.

Özalp, S., Emre, Ö., Duman, T.Y., Şaroğlu, F., Özaksay, V., Elmacı, H. and Koç, G. (2009) Çivril Graben Sistemi: Morfotektonik Yapısı ve Diri Fay Özellikleri, GB Türkiye. (Çivril graben system: Morphotectonic structure and active fault characteristics, SW Turkey). 62nd Geological congress of Turkey, pp. 804. (In Turkish)

Pourzarghan, V, Sarhaddi, H, Ramli, Z (2017) Morphology of ancient potteries using x-ray diffraction analysis and x-ray fluorescence in Sistan plain, eastern Iran. *Mediterranean Archaeology and Archaeometry*, Vol. 17, No 2, pp. 175-186.

Randive, K.R., Korakoppa, M.M., Muley, S.V., Varade, A.M., Khandare, H.W., Lanjewar, S.G., Tiwari, R.R. and Aradhi, K.K. (2005) Paragenesis of Cr-rich muscovite and chlorite in green-mica quartzites of Saigaon–Palasgaon area, Western Bastar Craton, India. *J Earth Syst Sci*, Vol. 124, No. 1, pp. 213-225.

Sarhaddi-Dadian, H., Zuliskandar, R., Nik Hassan Shuham, N. A. R., Mehrafarin, R. (2015) X-Ray Diffraction and X-Ray Fluorescence Analysis of Pottery Shards from New Archaeological Survey in South Region of Sistan, *Mediterranean,Archaeology and Archaeometry*, Vol 15, No. 3, 45-56.

Semiz, B. and Duman, B. (2017) Tripolis'te Bulunan Geç Antik Çağ Unguentariumlarının Arkeometrik Yönden Değerlendirilmesi (Archaeometric evaluation of Late Ancient Ages Unguentarium in Tripolis). in B. Duman, eds., Tripolis Ad Maeandrum I. pp. 165-180. (In Turkish)

Tolluoğlu, Ü. and Sümer, E. (1997) Afyon metasedimanter grubunda felsik metavolkanitlerin petrografik ve yapısal özellikleri (Petrographic and structural features of felsic metavolcanites in the Afyon metasedimentary group). Hacettepe University Earth Sciences, Vol. 19, pp. 57-70. (In Turkish)

Tolluoğlu, A.Ü., Erkan, Y., Sümer, E., Boyacı, M.N. and Yavaş, F.B. (1997) Afyon metasedimanter grubunun mesozoyik öncesi metamorfik evrimi (The Pre-Mesozoic metamorphic evolution of Afyon metasedimentary group). Geological Bulletin of Turkey, Vol. 40, No. 1, pp. 1-17. (In Turkish)

Türkteki, M. (2014) Early Bronze Age pottery manufacture in Western Anatolia: Identifying Hybrid Technologies through X-ray Analysis. Anatoliaca XL, pp. 93-109.

Yılmaz, Y., Genç, Ş.C., Gürer, F., Bozcu, M., Yılmaz, K., Karacık, Z., Altunkaynak, Ş. and Elmas, A. (2000) When did the western Anatolian grabens begin to develop?." in E. Bozkurt, J.A. Winchester, J.D.A. Piper, eds., Tectonics and Magmatism in Turkey and the Surrounding Area. Geological Society Special Publication, London: Blackwell, pp. 353-384.

Zimmermann, U., Kristoffersen, E.S., Fredriksen, P.D., Bertolino, A.A.R., Ando, S. and Bersani, D. (2015) Provenance and composition of unusually chrome and nickel-rich bucket-shaped pottery from Rogaland (southwestern Norway). Sedimentary Geology, Vol. 336, pp. 183-196.

Appendix 1. General archaeological characteristics of the settlements

1) Beycesultan Höyük (BYH): Beycesultan is the only settlement in Çivril Plain where the Middle and Late Bronze Age layers were studied through excavations. The site is located almost 100 km northeast of Denizli City and within the borders of Menteş and Kocakaya villages of southwestern Çivril district. The excavations have mapped architectural structures dated to the Early and Middle Bronze Ages expanding over an extremely wide area, together with several groups of important objects. Thus, this settlement remains the most significant data source of the region. On this double-coned mound, the first excavations were performed by J. Mellaart and S. Lloyd between the years 1954-1959 during 6 excavation season (Lloyd and Mellaart, 1962, 1965; Lloyd, 1972; Mellaart and Murray, 1995). The second period of excavation has been conducted by E. Abay since 2007 (Abay and Dedeoğlu, 2009, 2014). Samples from different ceramic groups dated to the Early Bronze Age II and Middle Bronze Age layers of the settlement are analyzed in this paper.

2) Aşağı Asartepe Settlement (AAS): This site is located 3 km east of Belence Village and 2 km southwest of Çapak Village, both in Çivril District. It is situated on a high and strategical natural hill almost 600 m north of the Küfü stream, possibily as a ness within the Küfü Valley. The ceramics indicate that the settlement was inhabited during the Middle Bronze Age, Iron Age, Hellenistic and Byzantine periods. In this paper, two sherds from the light brown coloured group dated to the Middle Bronze Age are analyzed.

3) Kocakaya Settlement (KS): The Kocakaya settlement is located within the borders of Belence Village in Çivril District, but about 3 km southwest of the village center. The mound is located in the Küfü Valley, on a west-east sloped natural hill on the west side of the Küfü stream. The Kocakaya Settlement is a typical hilltop settlement. Pottery dated to the Middle Bronze Age, Early Roman and Late Roman periods has been found at the settlement. A significant group of ceramics dates to the Middle Bronze Age, many of which are either brown or red-undercoated and polished. In this paper, samples from different ware groups of the Middle Bronze Age are analyzed.

4) İlimanlı Höyük (IH): İlimanlı Höyük is located in the neighborhood of İlimanlı Mevkii between Aşağı Çapak and Yukarı Çapak Villages within Çivril District. This site is situated on the west side of Kocaalan and Yukarı Asar Tepe and on the southeast side of the Taşçapak Settlement, on an east-west sloped piece of land. The İlimanlı Stream is on the very west side of the settlement, and the village road to Yukarı Çapak Village is located to its southeast. The settlement is situated on a natural hill and spreads out in a north-south direction. Ceramics dated to the Late Chalcolithic, Early Bronze Age I, Early Bronze Age III, Middle Bronze Age, Late Roman, Byzantine and Seljukian periods have all been found at this settlement. In İlimanlı Höyük, red and light-brown sliped bowl sherds with outward thickened rims and vertical handles date to the Middle Bronze Age. In this paper, one sample from the light-brown ware group dated to Middle Bronze Age is analyzed.

5) Belkuyu Höyük (BH): Belkuyu Höyük is located in the region with the same name, 3 km northwest of Çakallar Village and 3.5 km north of Köseler Village, both in Çivril District. This site is situated on a north-south sloped natural hill. The settlement, expanding mostly in the northwest-southeast directions, is surrounded by natural hills. Ceramics dated to the Early Bronze Age II, Middle Bronze Age, Early Roman, Late Roman, Byzantine and Seljukian periods have been found at the settlement. The Middle Bronze Age ceramics from the settlement are generally brown and red sliped bowls with thickened outward rims. In this paper, three Middle Bronze Age ceramics from the light-brown and brown ware groups are analyzed.

6) Çeşmebaşı Settlement (ÇS): The Çeşmebaşı Settlement is located within the borders of Nandallı village of Çivril District. The settlement, which is located 1.5 km southeast of Nandallı Village, is situated about 650 m southeast of the east-west trending dirt road that connects to the Çivril-Uşak main road. The settlement, located on an east-west trending natural hill, spreads over an extremely wide area, together with its cemetery. Its northern and western parts are surrounded by the Burgaz Mountain. Ceramics dated to the Middle Bronze Age, Early Roman and Byzantine periods have been found at the settlement. In this paper, three ceramics from the red and brown ware groups dated to the Middle Bronze Age are analyzed.

7) Cabar Asartepe Settlement (CAS): This settlement is located within Cabar Village in Çivril District, 3 km southeast of the village center. It is also 2200 m east of the Çivril-Uşak main road. The settlement is located

on a north-south trending natural hill with a view of the lowlands, within steep topography. Bedrock is exposed on the surface in many parts of the site. In the center of the settlement, few ceramics have been found. The ceramics at the settlement indicate that Cabar Asartepe was inhabited during the Early Bronze Age II, Middle Bronze Age, Iron Age, Hellenistic, Early Roman, Byzantine and Seljukian periods. The Middle Bronze Age ceramics analyzed in this paper belong to body sherds and bowls with outward thickened rims from light-brown and brown sliped ware groups.
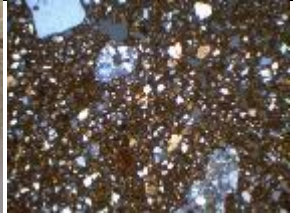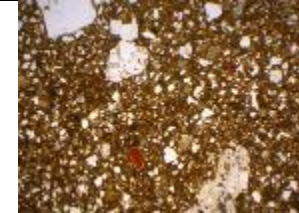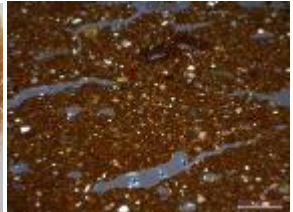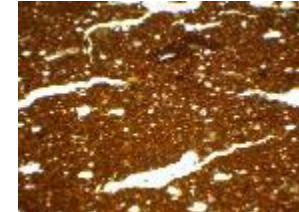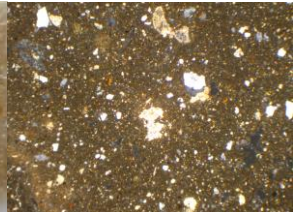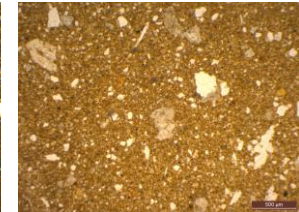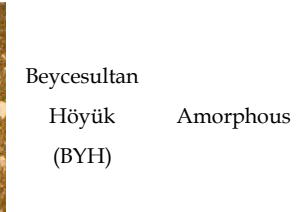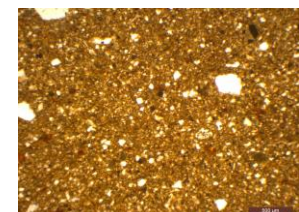
8) Göceler Höyük (GH): This settlement is located almost 1 km southwest of Göceler Village and 3 km southwest of Karalar Village. It is also located 2.5 km from the Dere Höyük Settlement and 2 km from the Karalar Settlement. The settlement is on a natural hill situated on a wide plane. The Burgaz stream flows by the western and southern sides of Göceler Höyük. This dry stream, dry for a significant time period, forms an extremely wide valley and a natural route. This route opens towards Çal-Banaz (Uşak) on the northeastern side and towards Çivril- Dinar (Afyon) on the eastern side. Early Bronze Age I and a lesser amount of Middle Bronze Age ceramics have been identified on the mound.
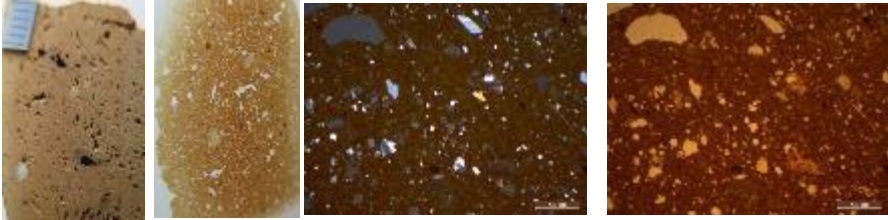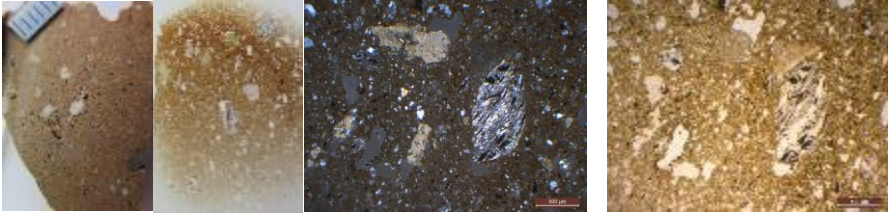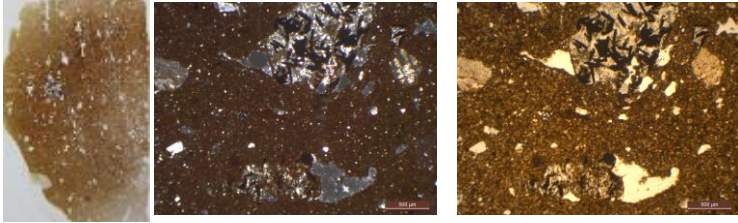
9) Höyük Settlement (HS): This settlement is situated almost 1 km southeast of Aşağı Seyit Village in Çal District near the Meander River. Stone enclosure walls located on the eastern and western sides of the mound seem to belong to different time periods and have different building techniques. Early Bronze Age I-II, Middle Bronze Age, Late Bronze Age and Iron Age ceramics were located during surveys of the settlement.
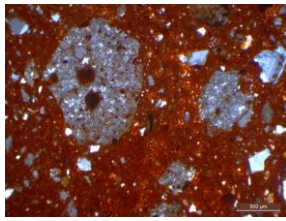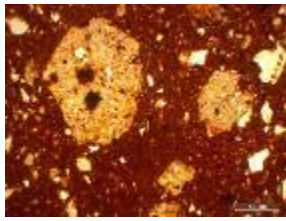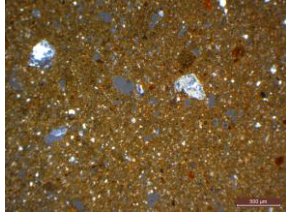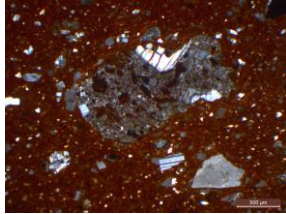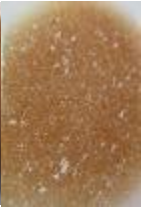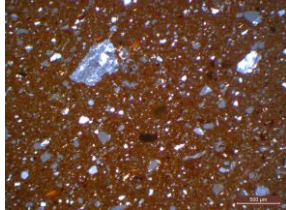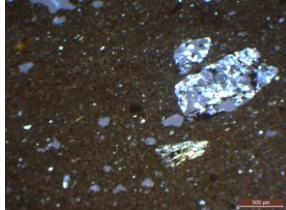
10) Asmakuyu Tepe Settlement (ATS): This settlement is located on a hill almost 3 km west of İmrallı Village, just on the edge of the valley. Due to this topography, it exhibits the identity of an uphill settlement. The hill on which the settlement is situated is at the intersection point of two valleys, one on the west and the other on the east. Thus, it is located between two valleys and the eastern side of the mound is a cliff face. These geographical features make the settlement a sheltered place. The remains of architectural structures indicate that the settlement was surrounded by enclosure walls. As a result of this research, it is understood that the settlement was only inhabited during the Early Bronze Age II.
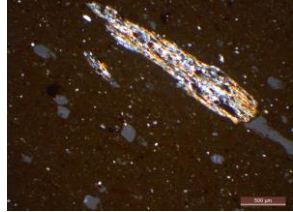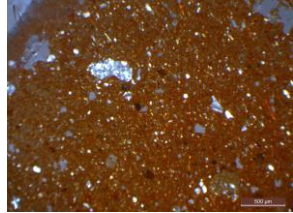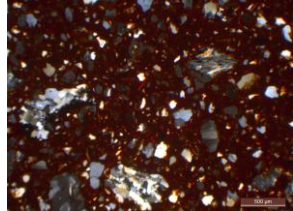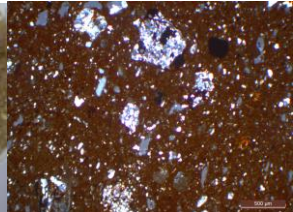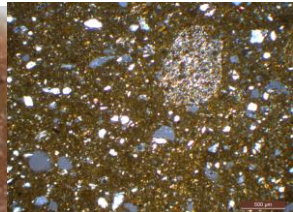
11) Kocainüstü Tepe Settlement (KTS): This settlement is 4 km from İmrallı Village on a hill situated on the road to Gömce. The settlement was founded on bedrock, where two deep valleys from the north and the south meet. Three sides of the settlement (east-south-north) are cliff faces, so the only way to submount the settlement is on the western side. Unidentified architectural structures on the settlement seem to indicate that the settlement was surrounded by fortification walls. As a result of the research on the settlement, a large amount of ceramics dated to the Early Bronze Age II has been found.
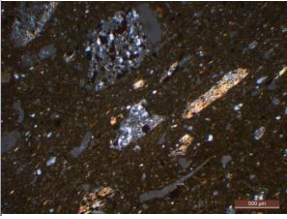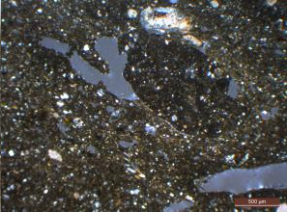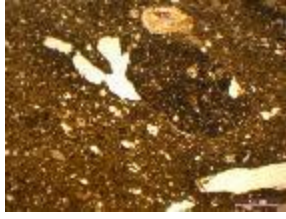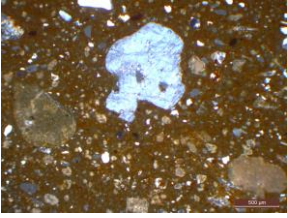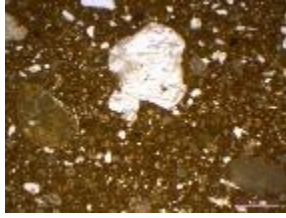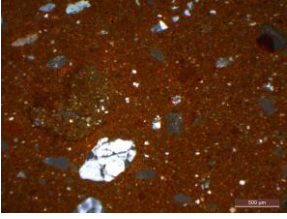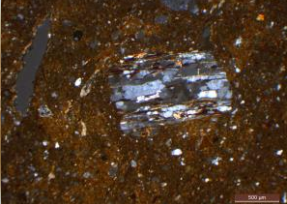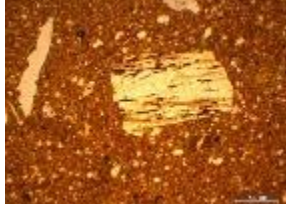
Appendix 2. General characteristics of the analyzed samples (Qtz:Quartz, Pl:Plagioclase, Cal:Calcite, Cpx:Pyroxene, Ms:Muscovite, Bi:Biotite, MRF:Metamorphic Rock fragments, OM:Optical microscopy, XRF: X-ray Fluorescence, XRD: X-ray powder diffraction) (abbreviations from Kretz, 1983).
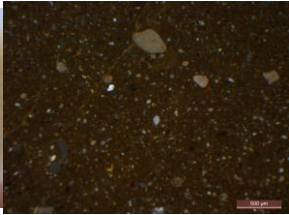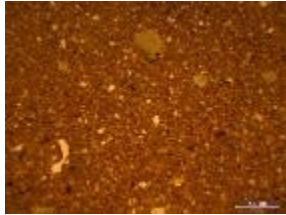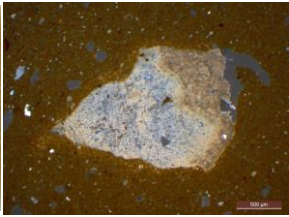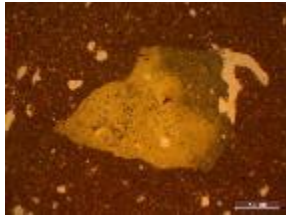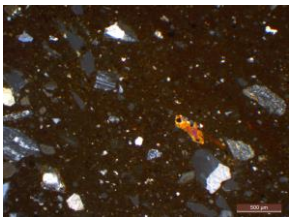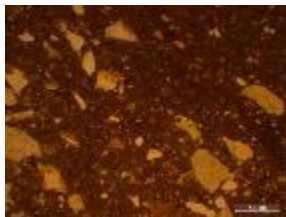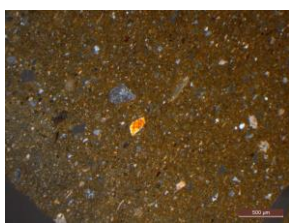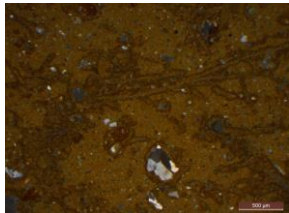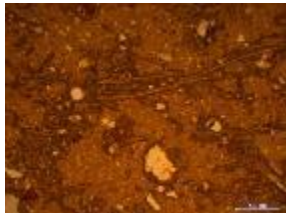
Sam code	Sample photo.	Sample photo.	Thin section (XPL)	Thin section (PPL)	Locations	Forms	Product class	Mineral Comp.	Period (century)	Analyses Methods	Groups
E01					Beycesultan Höyük (BYH)	Amorphous	Brown	Q, Pl, Bi, ±Ms, Cpx, Cal, ±MRF	Lowland Early Bronze Age-II	OM, XRF	Group1
E02					Beycesultan Höyük (BYH)	Amorphous	Brown	Pl, ±Q, Cal, Bi, Ms	Lowland Early Bronze Age-II	OM, XRF	Group1
E03					Beycesultan Höyük (BYH)	Amorphous	Brown	Pl, Bi, Q, Cal, ±MRF, Ms	Lowland Early Bronze Age-II	OM	Group1
E04					Beycesultan Höyük (BYH)	Amorphous	Brown	Pl, Q, Cpx, Cal, ±Ms, MRF	Lowland Early Bronze Age-II	OM	Group1
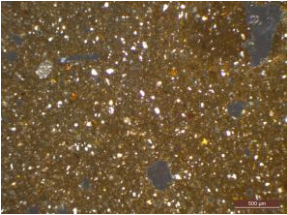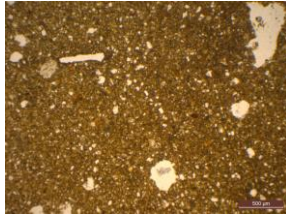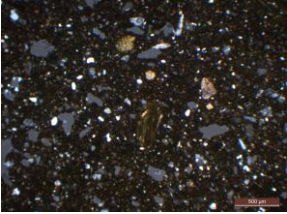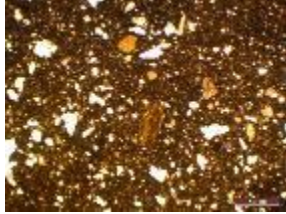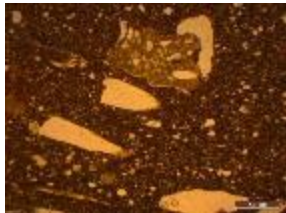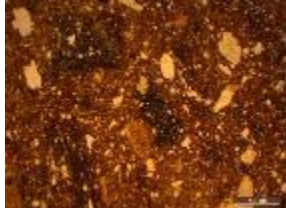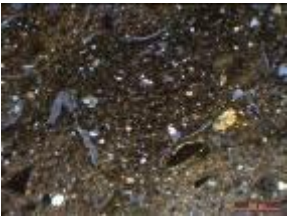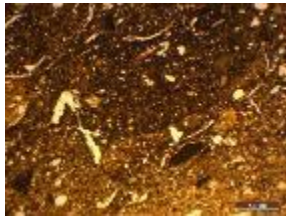
					Location	Form	Surface	Mineralogy	Age	Methods	Group
E05					Beycesultan Höyük (BYH)	Amorphous	Rough	Bi, Q, MRF, Pl, Cpx, ±MRF	Lowland Early Bronze Age-II	OM, XRF, XRD	Group1
E06					Aşağı Asartepe Settlement (AAS)	Amorphous	Brown	Q, Cal, MRF, Ms	Mountainous Middle Bronze Age	OM	Group3
E07					Aşağı Asartepe Settlement (AAS)	Amorphous	Brown	Q, Cal, Cpx, ±MRF	Mountainous Middle Bronze Age	OM	Group3
E08					Kocakaya Settlement (KS)	Handle	Brown	Q, Ms, MRF	Mountainous Middle Bronze Age	OM, XRF, XRD	Group3
E09					Kocakaya Settlement (KS)	Amorphous	Light brown	Q, Cal, MRF	Mountainous Middle Bronze Age	OM, XRF	Group3
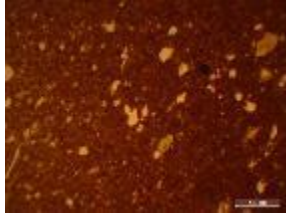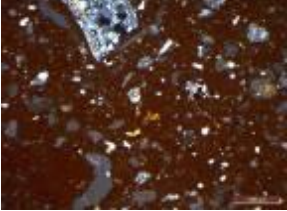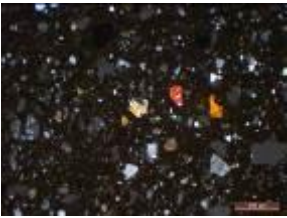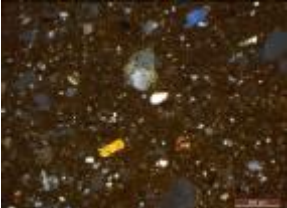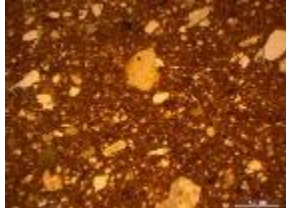
E10		Kocakaya Settlement (KS)	Amorphous	Light brown	Pl, Q, Amp, Bi, VRF, Cpx, ±MRF	Mountainous Middle Bronze Age	OM, XRF	Group2
E11		Kocakaya Settlement (KS)	Handle	Red	Q, MRF, Ms, ±Cpx, ±Cal	Mountainous Middle Bronze Age	OM, XRF	Group3
E12		İlimanlı Höyük (IH)	Amorphous	Dark brown	Q, Pl, Cpx, VRF, ±MRF	Mountainous Middle Bronze Age	OM	Group3
E13		Belkuyu Höyük (BH)	Amorphous	Brown	Q, ±Pl, Bi, ±MRF, Cal, ±Cpx	Mountainous Middle Bronze Age	OM	Group3
E14		Belkuyu Höyük (BH)	Amorphous	Light brown	Q, MRF	Mountainous Middle Bronze Age	OM	Group3
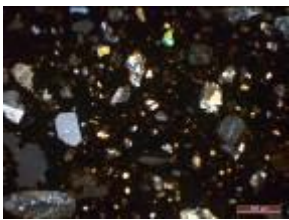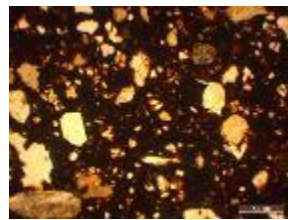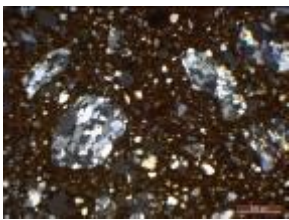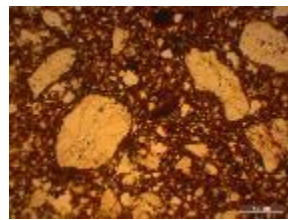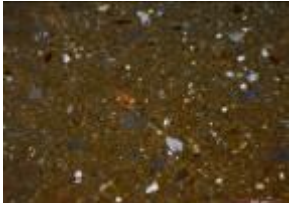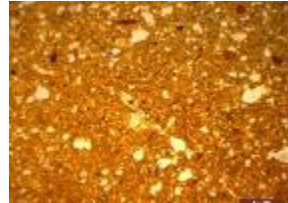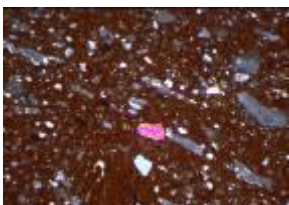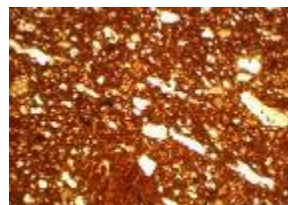
E15					Belkuyu Höyük (BH)	Amorphous	Brown	Cpx, Ms, MRF	Mountainous Middle Bronze Age	OM, XRF, XRD	Group3
E16					Çeşmebaşı Settlement (ÇS)	Amorphous	Red	Q, MRF, Ms, ±Cpx, Bi, Cal, Pl	Mountainous Middle Bronze Age	OM	Group3
E17					Çeşmebaşı Settlement (ÇS)	Amorphous	Red	Q, Pl, Cpx, MRF	Mountainous Middle Bronze Age	OM	Group2
E18					Çeşmebaşı Settlement (ÇS)	Amorphous	Brown	Q, Ms, MRF	Mountainous Middle Bronze Age	OM, XRF, XRD	Group3
E19					Cabar As-artepe Settlement (CAS)	Earthenware	Brown	Q, Ms, MRF	Mountainous Middle Bronze Age	OM	Group3
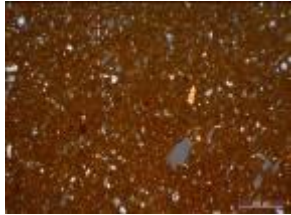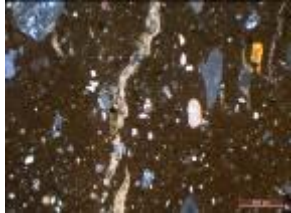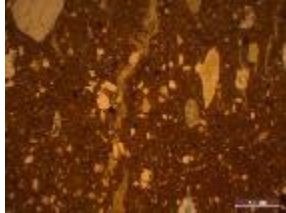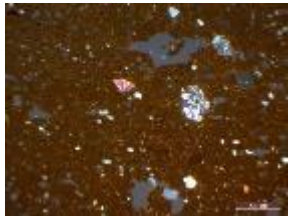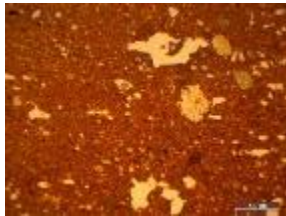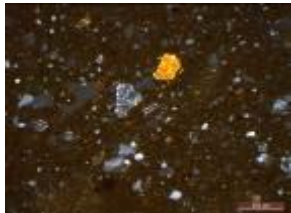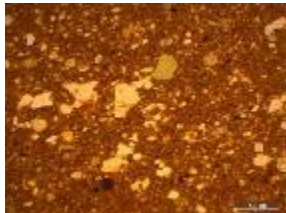
E20					Cabar As-artepe Set-tlement (CAS)	Bowl	Brown	Q, Cpx, Ms, MRF, Cal	Mountainous Middle Bronze Age	OM	Group3
E21					Cabar As-artepe Set-tlement (CAS)	Bowl	Light brown	Q, MRF, Cal	Mountainous Middle Bronze Age	OM	Group3
E22					Göceler Höyük (GH)	Bowl	Light brown	Q, Ms, ±Pl, Cal	Plateau Middle Bronze Age	OM	Group2
E23					Göceler Höyük (GH)	Amorphous	Red	Q, ±Cpx, MRF, Cal, ±Pl	Plateau Middle Bronze Age	OM, XRF	Group2
E24					Göceler Höyük (GH)	Amorphous	Brown	Q, Cal, Pl, ±Cpx, MRF	Plateau Middle Bronze Age	OM, XRF, XRD	Group2

E25		Höyük Settlement (HS)	Amorphous	Dark brown	Q, MRF, Bi, Cal, Cpx	Lowland Middle Bronze Age	OM	Group1
E26		Höyük Settlement (HS)	Amorphous	Dark brown	Q, Cal, ±cpx	Lowland Middle Bronze Age	OM	Group1
E27		Höyük Settlement (HS)	Amorphous	Grey	Cal, Q, Cpx, Pl, MRF	Lowland Middle Bronze Age	OM, XRF, XRD	Group1
E28		Höyük Settlement (HS)	Amorphous	Red	Q, Cpx, Pl, Bi	Lowland Middle Bronze Age	OM	Group1
E29		Höyük Settlement (HS)	Amorphous	Light brown	Q, MRF, Pl,	Lowland Middle Bronze Age	OM	Group1

E30		Asmakuyu Tepe Settlement (ATS)	Amorphous	Brown	Q	Mountainous Early Bronze Age-II	OM, XRF	Group1
E31		Asmakuyu Tepe Settlement (ATS)	Amorphous	Brown	Q, Pl, Cpx,	Mountainous Early Bronze Age-II	OM, XRF	Group2
E32		Asmakuyu Tepe Settlement (ATS)	Amorphous	Brown	Q, Cal, Pl	Mountainous Early Bronze Age-II	OM, XRF, XRD	Group2
E33		Kocainüstü Tepe Settlement (KTS)	Amorphous	Rough	Q, MRF	Mountainous Early Bronze Age-II	OM, XRF	Group3
E34		Kocainüstü Tepe Settlement (KTS)	Amorphous	Light brown	Q, MRF	Mountainous Early Bronze Age-II	OM, XRF, XRD	Group3

E35		Beycesultan Höyük (BYH)	Bowl	Brown	Q, MRF, Pl, Cpx,	Lowland Middle Bronze Age	OM	Group2
E36		Beycesultan Höyük (BYH)	Bowl	Brown	Q, Pl, Cpx, Amp,	Lowland Middle Bronze Age	OM, XRF, XRD	Group2
E37		Beycesultan Höyük (BYH)	Earthenware	Brown	Q, Pl, Cpx, MRF, Cal, Bi	Lowland Middle Bronze Age	OM	Group2
E38		Beycesultan Höyük (BYH)	Bowl	Silver mica lined	Q, Cpx, Pl, MRF, Cal	Lowland Middle Bronze Age	OM	Group2
E39		Beycesultan Höyük (BYH)	Bowl	Brown	Cpx, Q, MRF, Cal, Pl	Lowland Middle Bronze Age	OM	Group2

E40				Beycesultan Höyük (BYH)	Earthenware	Rough	Q, MRF, Cpx,	Lowland Middle Bronze Age	OM	Group2
E41				Beycesultan Höyük (BYH)	Earthenware	Rough	Q, MRF, Cal	Lowland Middle Bronze Age	OM	Group3
E42				Beycesultan Höyük (BYH)	Earthenware	Rough	Q, cpx	Lowland Middle Bronze Age	OM	Group3
E43				Beycesultan Höyük (BYH)	Pitcher	Red brown	Q, Cpx, Bi, Cal, Pl	Lowland Middle Bronze Age	OM, XRF	Group2
E44				Beycesultan Höyük (BYH)	Bowl	Red	Q, Bi,Pl, Cpx	Lowland Middle Bronze Age	OM	Group2

	Beycesultan Höyük (BYH)	Bowl	Red	Q	Lowland Middle Bronze Age	OM	Group2
E45							

E46	Beycesultan Höyük (BYH)	Bowl	Fallow	Q, MRF, Bi, Cal, Pl	Lowland Middle Bronze Age	OM, XRF	Group2

E48	Beycesultan Höyük (BYH)	Bowl	Gold paint lined	Cpx, Q, ±MRF	Lowland Middle Bronze Age	OM	Group2

E49	Beycesultan Höyük (BYH)	Orchard	Red	Q, Cpx, MRF, Pl,	Lowland Middle Bronze Age	OM, XRF, XRD	Group3